BIROn - **B**irkbeck **I**nstitutional **R**esearch **On**line

Enabling open access to Birkbeck's published research output

Characterisation of Bombyx mori odorant-binding proteins reveals that a general odorant-binding protein discriminates between sex pheromone components

Journal Article

http://eprints.bbk.ac.uk/1024

Version: Accepted (Refereed)

Citation:

© 2009 Elsevier

Publisher Version

Deposit Guide

Contact: lib-eprints@bbk.ac.uk

Characterisation of *Bombyx mori* Odorant-Binding Proteins Reveals that a 'General Odorant-Binding Protein' Discriminates Between Sex Pheromone Components

Jing-Jiang Zhou[1*], Giles Robertson[2], Xiaoli He[1], Samuel Dufour[1], Antony M. Hooper[1], John A. Pickett[1], Nicholas H. Keep[2] and Linda M. Field[1]

[1] *Department of Biological Chemistry, Rothamsted Research, Harpenden, AL5 2JQ, UK*
[2] *School of Crystallography, Institute for Structural and Molecular Biology, Birkbeck College, University of London, London, WC1E 7HX, UK*

*Corresponding author: Jing-Jiang Zhou, Department of Biological Chemistry, Rothamsted Research, Harpenden, AL5 2JQ, UK. Tel.: +44 (0)1582 763133, Fax: +44 (0)1582 762595, email: jing-jiang.zhou@bbsrc.ac.uk

Classification: Protein and nucleic acid structure, function and interactions.

Running title: *Bombyx mori* odorant-binding proteins

Abbreviations: PBP, pheromone-binding protein; GOBP, general odorant-binding protein; ABP, antennal binding protein; OR, olfactory receptor.

Summary

In many insect species odorant-binding proteins (OBPs) are thought to be responsible for the transport of pheromones and other semiochemicals across the sensillum lymph to the olfactory receptors (ORs) within the antennal sensilla. In the silkworm *Bombyx mori* the OBPs are subdivided into three main subfamlies, pheromone-binding proteins (PBPs), general odorant-binding proteins (GOBPs) and antennal binding proteins (ABPs). We used the 'MotifSearch' algorithm to search for genes encoding putative OBPs in *B. mori* and found 13, many fewer than are found in the genomes of fruitflies and mosquitoes. The 13 genes include seven new *ABP*-like *OBPs* as well as the previously identified *PBPs* (three), *GOBPs* (two) and *ABPx*. Quantitative examination of transcript levels showed that *BmorPBP1, BmorGOBP1*, *BmorGOBP2* and *BmorABPx* are expressed at very high levels in the antennae and so could be involved in olfaction. A new two-phase binding assay, along with other established assays, showed that BmorPBP1, BmorPBP2, BmorGOBP2 and BmorABPx all bind to the *B. mori* sex pheromone component (10*E*,12*Z*)-hexadecadien-1-ol (bombykol). BmorPBP1, BmorPBP2 and BmorABPx also bind the pheromone component (10*E*,12*Z*)-hexadecadienal (bombykal) equally well, whereas BmorGOBP2 can discriminate between bombykol and bombykal. X-ray structures show that when bombykol is bound to BmorGOBP2 it adopts a different conformation from that found when it binds to BmorPBP1. Binding to BmorGOBP2 involves hydrogen bonding to Arg110 rather than to the Ser56 as found for BmorPBP1.

Introduction

In insects odorant-binding proteins (OBPs) provide the initial molecular interactions for chemical signals (semiochemicals) such as pheromones and host odours and are thought to ferry the semiochemical molecules across the antennal sensillum lymph to the olfactory receptors (ORs). The involvement of pheromone-binding proteins (PBPs) and general odorant-binding proteins (GOBPs) in recognising and transporting pheromones and host odours is supported by the findings that they are highly concentrated (up to 10 mM) in the lymph of chemosensilla, that some are expressed specifically in antennae and that the distribution of the different subfamilies of OBPs is related to specific functional chemosensilla. [1,2,3,4,5,6,7,8]

All insect OBPs have six highly conserved cysteine residues [9,10] which form disulphide bridges stabilising the 3D structure. [11,12,13] This sequence motif has been used for genome-wide identification and annotation of OBP genes in a range of insect species. [14,15,16,17] Based on their sequence and their expression patterns in male and female antennae, OBPs in lepidopteran species are usually divided into different subfamilies; the PBP [18], the GOBP [9,18,19] and the antennal binding protein X homologues (ABPx). [20] PBPs of Lepidoptera are either specific to, or highly enriched in, the antennae of male moths and have been shown to bind the sex pheromones produced by females. [2,21,22] However, PBPs have also been found in the antennae of females and in male sensilla which are not pheromone-sensitive. [20,23,24,25,26] GOBPs are usually expressed equally in the antennae of both sexes consistent with a proposed role in the detection of host volatiles. [3,20,25,27,28,29,30] ABPxs display limited sequence homology to PBPs and GOBPs but have the same sequence motif of the conserved cysteine residues as PBPs and GOBPs. [20] No specific role has yet been proposed for them.

Although it has been shown *in vitro* that OBPs can facilitate the passage of semiochemicals to the ORs, where the response of the insect to the chemical signal is initiated [31,32,33,34,35,36], there is no conclusive evidence showing this *in vivo.* Thus the exact functional roles that these proteins play in insect olfaction remain unclear. In at least one case, the

ligand-OBP complex may activate the OR directly rather than by releasing the odorant molecule to the OR. [37]

In the silkworm *Bombyx mori*, four putative PBPs and five GOBPs have been observed by iso-electric focussing and mobility in native gel electrophoresis and *N*-terminal microsequencing. [27,38] The PBP, BmorPBP1, was first isolated from male antennae [39] and the corresponding gene was cloned, together with genes for BmorGOBP1, BmorGOBP2 and BmorABPx, by screening a male antennal cDNA library. [20] BmorGOBP2 was found to be expressed at a very high level in the long sensilla of female moths. [21] BmorPBP1 and its binding to pheromone components have been the subject of intense study in recent years as a model system for understanding the functions that OBPs may play in insect olfaction. [40,41,42,43,44,45,46] Cells expressing BmorPBP1 are closely associated with the cells expressing BmorOR-1 and BmorOR-3 in the long sensilla. [8,47] Co-expression of BmorPBP1 with BmorOR-1 in an 'empty' neuron of *Drosophila melanogaster* [48] increased sensitivity of the receptor to the sex pheromone component (10*E*,12*Z*)-hexadecadien-1-ol (bombykol). [33] BmorPBP1 has also been shown to mediate a response to bombykol but not to another pheromone component (10*E*,12*Z*)-hexadecadienal (bombykal) in cultured HEK 295 cells expressing BmorOR-1. [34] The authors also proposed that there was another unidentified PBP responsible for mediating the bombykal response observed in the long sensillum. [34] They have recently identified two additional *PBP* genes encoding BmorPBP2 and BmorPBP3 but neither protein is co-expressed with BmorPBP1 and BmorOR-1 in the long sensilla. [49]

Pheromones are usually blends of chemicals specific to a species and for *B. mori* the pheromone blend comprises bombykol, bombykal and (10*E*,12*E*)-hexadecadien-1-ol. [50] However, only bombykol is able to induce mating behaviour at a physiological concentration and bombykal acts as an antagonist to bombykol. [50,51] Binding of BmorPBP1 to bombykol has been demonstrated by X-ray crystallography, [13] NMR structural characterisation, [43,44,46] electrospray-mass spectrometry (ESI-MS) [52,53] and other biochemical methods. [40,42] It has been shown that the binding is both pH and ligand dependent. [43,44] At acidic pH, or in the

4

absence of bombykol, the C-terminus forms an α-helix and occupies the ligand binding pocket [44,45,46] and a conformational change brought about by a change in pH to more acid near the ORs is thought to be the ligand release mechanism when the BmorPBP1-bombykol complex reaches the ORs. [43,44,54,55] There is some evidence that BmorPBP1 can bind to both bombykol and bombykal. [56] However, ligands may be utilising very different molecular interactions when they bind to an OBP, which may influence the conformational properties of the OBP/ligand complex. [37] In this study we set out to annotate all possible OBP genes in the *B. mori* genome, examined the tissue expression patterns of six of the genes from three subfamilies and studied the binding of recombinant OBPs to the sex pheromone component bombykol and its analogues using a new two-phase binding assay and a competitive binding assay with a fluorescent probe. As a consequence of this work we also investigated the crystal structures of BmorGOBP2 complexed with bombykol and the analogues.

Results

Identification of OBPs in the *Bombyx mori* genome and EST libraries

To identify putative OBPs in the *B. mori* genome (21,302 peptide sequences) and EST libraries (245,762 ESTs) we utilised our in house developed MotifSearch algorithm. [17] In this case we combined the sequences motifs used previously for Classic and Atypical OBPs of *D. melanogaster* and *Anopheles gambiae*. [14, 17] Thus the sequence motifs used in the MotifSearch algorithm are C1 X15-39 C2 X3 C3 X21-38 C4 X7-15 C5 X8 C6, and C1 X8-41 C2 X3 C3 39-47 C4 X17-29 C4a X9 C5 X8 C6 X9-11 C6a for Plus-C OBPs. The sequences identified by the MotifSearch were BLASTp searched against known OBP sequences in the GenBank. The sequences with E-value of less than 10^{-6} to any known OBP sequences and with less than 9 cysteine residues were selected. Other OBP features such as molecular weight, pI and signal peptide were also used. The MotifSearch algorithm and BLAST identified 13 putative OBP genes. No additional PBPs and GOBPs were found apart from the previously identified *BmorPBP1, BmorPBP2, BmorPBP3, BmorGOBP1, BmorGOBP2*. [20,49] However, seven

BmorABPx homologues (*BmorOBP1*, *BmorOBP2, BmorOBP3, BmorOBP4, BmorOBP5, BmorOBP6 and BmorOBP7*) were found. The deduced protein sequences and the alignment of these sequences are presented in Figure 1 and the data were used to construct a phylogenetic tree (Figure 2) which clusters the sequences into three distinct groups; PBPs, GOBPs and ABPs. The seven new OBPs are clustered with ABPx. The total number of 13 OBPs for *B. mori* is much less than that found in *Anopheles gambiae* (66) and *D. melanogaster* (49) [17], but is comparable to the numbers found in the honey bee *Apis melifera* [57] and the pea aphid *Acyrthosiphon pisum* (unpublished).

Expression of *Bombyx mori* OBPs

The levels of transcripts of six *B. mori* OBPs, *BmorPBP1*, *BmorPBP2*, *BmorPBP3*, *BmorGOBP1*, *BmorGOBP2* and *BmorABPx* in adult moth tissues were measured using qRT-PCR. The measurements were carried out using two internal controls, an elongation factor and an actin. Results with the elongation factor are shown in Figure 3 and similar results were obtained with actin (data not shown). In general the levels of transcripts were very low in all tissues except in antennae where *BmorPBP1, BmorGOBP1, BmorGOBP2* and *BmorABPx* were highly expressed. These results are consistent with the high levels of the proteins encoded by these genes found in antennae by Western blot analysis and immunocytochemical labelling experiments. [2,21] Our results also show very low and insignificant transcript levels for *BmorPBP2* and *BmorPBP3* in all tissues in agreement with previous findings using *in situ* hybridisation. [49] Thus our data show that at least one member of each phylogenetic cluster of *B. mori* OBPs is expressed at high levels in the antennae and could therefore be involved in detection of odour ligands.

Competitive binding of ligands to *Bombyx mori* OBPs

Displacement of the fluorescent probe N-Phenyl-1-naphthylamine (NPN) has been used previously to assess binding of ligands to insect OBPs [22,58] and the fluorescence emission of BmorGOBP2 in the presence of NPN is shown in Figure 4. The intrinsic fluorescence of the

single tryptophan in BmorGOBP2 shows a strong blue shift (330 nm) compared to tryptophan in solution (348 nm) in the absence of NPN, indicating that the tryptophan is buried in the core of the protein. The binding of NPN to BmorGOBP2 reduces the intrinsic fluorescence emission of the tryptophan at 330 nm and initiates a new emission peak at 395 nm, indicating the bound NPN lies close to the tryptophan, as there is resonance energy transfer from the tryptophan resulting in the increase in the NPN fluorescence at 395 nm. This is also true for the other OBPs (data not shown). The displacement of NPN by ligands leads to a loss of the emission at 395 nm. We measured the NPN displacement for five of the *B. mori* OBPs (BmorPBP1, BmorPBP2, BmorGOBP1, BmorGOBP2, BmorABPx) by bombykol and four of its analogues bombykal, (10*E*,12*Z*)-tetradecadien-1-ol, (8*E*,10*Z*)-hexadecadien-1-ol and (10*E*)-hexadecen-12-yn-1-ol (for the synthesis of these compounds see Supplementary Figure 1). 1-Hexadecanol was also used as a control. The results of the fluorescence displacement are shown in Figure 5 and the differences between displacement of NPN by bombykol and bombykal for *B. mori* OBPs are summarised in Figure 6. This shows that it is only for BmorGOBP2 that bombykol can displace more NPN from the binding pocket than can bombykal. The differential NPN displacement from BmorGOBP2 by bombykol and bombykal increased with increased ligand concentration (Figure 5A) with a reduction in NPN fluorescence of 59.3±3.1% (n=4) by bombykol and 19.9±0.5% (n=2) by bombykal at the highest ligand concentration (7 uM) (Figure 6). For BmorPBP1 there was no difference in binding between bombykol and bombykal with the reductions of the NPN fluorescence being 57.0±2.3% (n=5) and 51.8±2.8% (n=2), respectively, at 7 uM (Figure 6). Both BmorPBP2 and BmorABPx bound bombykol and its analogues with much less discrimination. The change of the functional group from an alcohol in bombykol to an aldehyde in bombykal or from double bond in bombykol to a triple bond in (10*E*)-hexadecen-12-yn-1-ol and the removal of double bonds (1-hexadecanol) almost abolished the NPN displacement (Figure 5A). However, there was no significant difference in the displacement between bombykol and (8*E*,10*Z*)-hexadecadien-1-ol, and the shorter molecule (10*E*,12*Z*)-tetradecadien-1-ol decreased the NPN fluorescence to 59.3±2.8% (n=4).

Non-fluorescent assays of ligand binding to *Bombyx mori* OBPs.

We first tested the ability of BmorPBP1 to bind to bombykol and the control ligand 1-hexadecanol, alone or mixed together, using a cold binding assay. [40] There was no difference in binding to these two structurally different compounds when they were tested alone but when they were mixed there was discrimination between the ligands i.e. more bombykol than 1-hexadecanol was detected bound to BmorPBP1 (data not shown). Therefore, all subsequent binding experiments were carried out using mixtures of ligands. All of the *B. mori* OBPs tested bound to bombykol and its four analogues but the BmorGOBPs and BmorABPx bound better than did BmorPBP1 (Figure 7A). There was also no difference between the binding of bombykol and bombykal to BmorPBP1, consistent with our competitive binding results and those of others. [56]

In this cold binding assay, ligands could be released from the binding pocket during the washing step when the equilibrium is broken. We therefore developed a 'two-phase' binding assay. In this the protein in buffer is incubated with a mixture of ligands dissolved in hexane in two phases. Depletion of ligands from the top phase was measured by GC and compared with a control. The results for the five *B. mori* OBPs and five ligands are shown in Figure 7B. Again there is no significant difference in the binding of bombykol and bombykal to BmorPBP1, BmorPBP2 or BmorABPx but BmorGOBP2 did bind more to bombykol than to bombykal.

X-ray structure of BmorGOBP2.

The structure of BmorGOBP2 was solved in the presence of bombykol, bombykal, (8*E*,10*Z*)-hexadecadien-1-ol, (10*E*)-hexadecen-12-yn-1-ol, (10*E*,12*Z*)-tetradecadien-1-ol and no added ligand (Table 1). The BmorGOBP2/ligand complexes crystallised in two related crystal forms differing in the length of the c axis with bombykol and (10*E*)-hexadecen-12-yn-1-ol structures with a c axis of 189 Å and the other structures with a c axis of 172Å (Table 1). There is a greater root mean square deviation (RMSD) for Cα-atoms of matched residues

between the complexes from the different cell dimensions than within a group (e.g. bombykol/bombykal=0.52 Å over 139 residues; bombykol/(10*E*)-hexadecen-12-yn-1-ol =0.13 Å over 141 residues). The differences lie in the regions of amino acids 39-41, 62-66, 104-106, 123-128 and the C-terminus 139-141 (Figure 8A). These changes are of a similar size to those reported [37] as being responsible for the activation of the OBP LUSH of *D. melanogaster*, where the breaking of the salt-bridge between Lys87 and Asp118 either by addition of ligand 11-*cis*-vaccenyl acetate (cVA) or by mutation of Asp118 to Ala118 conferred activation of pheromone-sensitive neurons in a stimulation assay. However, inspection of all of the loops that differ in the BmorGOBP2 structures shows that they are involved in crystal contacts in one or both forms so the conformational changes may not have physiological significance.

The structure of BmorPBP1 with bombykol (PDB ID: 1DQE) [13] was the only previous OBP structure that gave a marginal solution calculated with PHASER. [59] The RMSD of Cα-atoms is 1.6 Å over 120 of 137 residues after refinement. The most significant differences between BmorGOBP2 and BmorPBP1 are at the C-terminus and in the second helix (Figure 9A). In BmorGOBP2 the longer C-terminal tail forms a regular amphipathic alpha helix that packs across the top of the N-terminal helix whereas in the BmorPBP1 complex with bombykol the C-terminus inserts between the first and second helices to close off the binding pocket. [13,43,44,45] The region equivalent to the second helix of BmorPBP1 is not a regular helix and the backbones of the two proteins take a completely different path between amino acid residues 29 and 37 including a bulge of residues 33-35 in BmorGOBP2 that occupies the position of the C-terminus in the BmorPBP1 structure. Probably the most significant residue in the structural change is Phe41 in BmorGOBP2 which is much more deeply buried in the protein than is Tyr41 in BmorPBP1 and occupies the space of the last turn of the second helix in BmorPBP1 (Figure 9A). In contrast the side chain of Tyr41 of BmorPBP1 interacts with the side chain of Asp32 which reinforces the second helix in BmorPBP1. The equivalent of position 41 is also a phenylalanine in BmorGOBP1 but a

tyrosine in all of the PBPs, indicating that this is a major distinction between the two subfamilies (Figure 1).

X-ray analysis of ligand binding to BmorGOBP2.

Inspection of the difference maps of the BmorGOBP2 structures revealed evidence of tubular density in their hydrophobic cavities. In the structure with no added ligand, the C-terminus does not occupy the binding site as seen with BmorPBP1, but this was only achieved with BmorPBP1 either at low pH or after exhaustive removal of the substrate from the binding site. [43,44,45,46]. The quality of the ligand density was generally poorer than that for the protein as a whole probably reflecting a degree of conformational flexibility as well as possible partial occupancy of the co-crystallised ligands. The Bfactors for the ligands are significantly higher than for the protein, reflecting the conformational flexibility of the ligand within the binding site. In the case of the bombykol structure this is 29.0 as opposed to 14.7 for the protein. The ratios of these values are comparable to other OBP structures for example with that of BmorPBP1 with bombykol [13] (1dqe) where the average ligand B factor is 40.0 compared to the protein average of 25.3 or for LUSH with 11 cis-vaccenyl acetate [37] (2gte) where the ligand B factor is 24.8 compared to a protein B factor of 10.9. For the other GOBP2 ligand complexes in this paper the ligand B factors are higher, probably reflecting partial occupancy as well as conformational flexibility as these ligands bind with lower affinity.

The most striking feature of the BmorGOBP2/ligand complexes is that the conserved Ser56 residue does not appear to take part in hydrogen bonding to the ligands in contrast to the bombykol bound structure of BmorPBP1. [13] Instead, each examined ligand appears to make some kind of interaction with Arg110. In all structures the ligand density although not of the highest clarity is clearly directed towards Arg110 and not Ser56 (Figure 9B,C). This residue is conserved as arginine in BmorGOBP1, BmorGOBP2, BmorPBP2 and BmorPBP3 (and BmorOBPs 4, 5 and 6) but interestingly is a tryptophan in BmorPBP1 (Figure 1). The interaction with Arg110 involves hydrogen bonding from the polar head group of the ligands to the epsilon amide of the arginine. However, it is not clear whether this interaction always

occurs directly, or is propagated through a water molecule. There is fairly unambiguous density supporting the role for a water molecule in the structures with (10*E*,12*Z*)-tetradecadien-1-ol, (8*E*,10*Z*)-hexadecadien-1-ol and (10*E*)-hexadecen-12-yn-1-ol. However, in the bombykol and bombykal bound structures the density is less clear cut and in the case of bombykol both conformations have been modelled as equally valid interpretations of the density. The Arg110 residue is present in a mixture of two conformations, to a greater or lesser extent depending on the nature of the ligand present. One conformation presents the epsilon amide of Arg110 for hydrogen bonding within the pocket, and is the major conformation for the bombykol complex. In the other conformation the guanidine group of Arg110 is flipped inwards occupying more space in the protein interior. Based on likely bonding distances, the second conformation is not involved in hydrogen bonding to water or directly to ligand and may represent the unliganded fraction. This second conformation is dominant in the ligand free structure and is more prevalent in the more weakly binding ligands than in the bombykol complex indicating that there is probably partial occupancy of the ligand site in these cases.

The extended interaction via a water molecule makes the formation of an additional hydrogen bond to Glu98 possible. This residue has been suggested as being of importance in molecular dynamics studies of ligand binding in BmorPBP1. [55,56] In this study a hydrogen bonding network involving the side chain of Glu98 and the main chain amide of Leu68 is implicated in a conformational change allowing ligand release via loss of restraint of the beta II turn region of the molecule when ligand competes for hydrogen bonding to Glu98. The beta II turn is a structural feature conserved in BmorGOBP2 as is a hydrogen bond to the amide of residue 68 (a methionine in BmorGOBP2). The bombykal polar group is an aldehyde and as such it is only able to accept hydrogen bonds. This is in contrast to the hydroxyl groups of the other ligands that are able to both accept and donate. This might be a significant feature as bombykal would not be able to form the additional hydrogen bond to Glu98 unless that residue was protonated. However, given that the pH of crystallisation is 8.5

this may be unlikely. The loss of such a bonding interaction might explain the differences observed in binding between bombykal and bombykol.

Discussion

The transcripts of *BmorPBP1*, *BmorGOBP1*, *BmorGOBP2* and *BmorABPx* are highly expressed in antennae and when recombinant proteins from these genes were studied all but BmorGOBP1 bound the sex pheromone bombykol and its analogues. It is possible that BmorGOBP1 is an inactive allelic variant as reported in *Manduca sexta.* [25] Both the competitive binding assay and non-fluorescent binding measurements showed a broad and overlapping ligand spectrum for all of the OBPs and therefore they could transport any of the three known pheromone components to the ORs in the chemosensilla. However, there is evidence from the binding studies that BmorGOBP2 can discriminate between the sex pheromone components bombykol and bombykal. It is possible that the combinatorial actions by OBPs and ORs may provide the foundation for insects to discriminate various odorants as reported in mammalian species. [60,61]

For the first time we report X-ray structures of BmorGOBP2 complexed with bombykol and four of its analogues. Although there are some significant structural differences between BmorGOBP2 and BmorPBP1, in particular in the region of the second helix, most of the main contributors to the ligand binding pocket are conserved. However, the mode of bombykol binding to BmorGOBP2 differs from that found for BmorPBP1. In BmorGOBP2 the hydroxyl hydrogen of bombykol forms a hydrogen bond to Arg110 probably via a water molecule, whereas in BmorPBP1 its hydrogen binds to Ser56. Within the *B. mori* OBPs it is BmorPBP1 that is the outlier having a tryptophan in the place of Arg110 found in most other OBPs. The GOBPs differ from the PBPs at residue Phe41 where the PBPs have a tyrosine. It is proposed from molecular dynamics studies [55,56] and 3D structures of BmorPBP1 [13,43,44,62] that there are two modes of bombykol entry and exit from the binding pocket the so called front and back exits. The front exit involves the opening of the flap formed by residues 60-68

which is thought to be controlled by the His69, His70 and His95. These residues are conserved throughout the GOBPs and PBPs. We see involvement of Glu98 in binding ligands in the resting state in BmorGOBP2. This residue is conserved in all the *B. mori* GOBPs and PBPs except BmorPBP2 where it is a serine. Glu98 in BmorPBP1 is proposed to provide an intermediate hydrogen bond on the front binding pathway [55] and is hydrogen bonded to His95, one of the residues that controls the opening of the flap. This potentially allows ligand binding to control the opening of the pocket and is a mechanism of communicating ligand binding to the exterior surface of the protein. His95 is in multiple conformations in the BmorGOBP2 complexes with bombykal, (10*E*,12*Z*)-tetradecadien-1-ol, (8*E*,10*Z*)-hexadecadien-1-ol and the structure without added ligand but this may be an effect of crystal packing. The back exit involves the opening blocked by the C-terminus of the BmorPBP1/bombykol structure but not in the structures with the non-natural ligands 2-isobutyl-3-methoxypyrazine and iodohexadecane. [62] In the BmorGOBP2 structure this opening is blocked by amino acid residues 33 to 35, which probably means that this second mode of entry is not available, as the basis of this conformational difference is hydrophobic packing of Phe41 which is unlikely to undergo movements that open this pocket. It should however be noted that closure of the binding pocket is not necessary for ligand binding as structures of BmorPBP1 with 2-isobutyl-3-methoxypyrazine and iodohexadecane [61] have a disordered C-terminus and the pocket remains accessible.

Recently an alternative model of activation where the OBP-ligand complex interacts with the olfactory receptor has been proposed based on conformational differences in the crystal structure of the *D. melanogaster* OBP LUSH with its physiological ligand compared to other ligands. In LUSH conformational changes on the activating ligand (cVA) binding lead to the breaking of the salt bridge between Lys87 and Asp118. Mimicking of this salt bridge disruption in the D118A mutant gave a mutated protein that would constitutively activate T1 neurons when the receptor Or67d was present without the need for ligand. The conformational shift is thought to be driven by movements of Phe121 in the C-terminus. [37] In BmorGOBP2 there is a structurally analogous salt bridge to that in LUSH, between Lys89

and Glu125. This is extended in the bombykol structure to 3.4 Å compared to 2.9Å in the bombykal structure but is certainly not broken. We see other conformational changes of a similar magnitude between the BmorGOBP2/bombykol and bombykal structures but cannot rule out these being purely due to crystal packing differences.

In the honey bee PBP ligand binding is dependent on a low pH and protonation of Asp35 which locks down the C-terminus in a conformation that closes the active site by a hydrogen bond to the main chain of Val118. [63] In BmorPBP1/bombykol structure the C-terminus blocks the rear entry to the pocket with Val135 coming within 4Å of bombykol. However, it is not immediately apparent why this interaction is not reiterated in the complex with iodohexadecane as there is similar exposure of the aliphatic chain for Val135 to interact with. [44, 62]   Therefore there is a possible theme with LUSH, BmorPBP1 and the bee PBP having the C-terminus responding in a different manner to physiological ligands than to non-specific ligands. However, with BmorGOBP2 due to the blocking of the rear pocket by the bulge formed by amino acid 33-35 the C-terminus cannot sense the ligand directly.

Our data do not agree with previous suggestions that BmorPBP1 is specific for bombykol and that BmorGOBP2 is involved in detection of plant volatiles as predicted by the immunochemical localisation. Instead we find that both proteins bind to bombykol and bombykal. Our studies also show that BmorGOBP2 binds differently to bombykol and bombykal in both a fluorescent competitive binding assay and non-fluorescent binding measurements. The structural evidence would indicate that lack of hydrogen bonds to Glu98 may be the source of this discrimination. This suggests that BmorGOBP2 may also have a role in pheromone perception as bombykol is a stronger stimulant than bombykal.

Materials and Methods

Identification of *Bombyx mori* sequences containing OBP Motifs.

The whole genome peptide sequences of *B. mori* were downloaded from the Silkworm knowledgebase (http://silkworm.genomics.org.cn/jsp/download.jsp) and the EST sequences were retrieved from the NCBI EST database (http://www.ncbi.nlm.nih.gov/dbEST/) and searched using the OBP 'MotifSearch' program described previously. [14,15,16,17] The OBP sequences identified were aligned using Clustal X (8.1) [64] with default gap-penalty parameters of gap opening 10 and extension 0.2. The phylogenetic tree was then constructed from the multiple alignments using MEGA 4 software. [65] The final unrooted consensus tree was generated with 1500 bootstrap trials using the neighbour-joining method [66] and presented with a cut off value of 70.

Quantitative RT-PCR (qRT-PCR).

B. mori cocoons were kindly provided by Prof. YP Haung (Institute of Plant Physiology and Ecology, CAS, China) and adult moths were dissected immediately after hatching into antennae, heads, legs, wings and the remaining 'bodies'. Each tissue was ground in liquid nitrogen and total RNA extracted using RNAqueous kit (Ambion) and treated with DNaseI (Sigma). Two step real time RT-PCR was carried out with the ETROscript kit according to the manufacturer's protocol (Ambion). Before qRT-PCR, normal RT-PCRs were done with each primer pair using Hotstart Taq DNA polymerase (Qiagen) and the products were run on 1% agarose gels and stained with ethidium bromide to check that the correct products were being amplified. The PCR primers were designed with Primer3 (http://frodo.wi.mit.edu/) and were: Actin 5'-CGTTCGTGACATCAAGGAGA-3' and 5'-ACAGGTCCTTACGGATGTCG-3'; Elongation factor 5'-CGATGGAAAGGTGCTCCTAA-3' and 5'-TGACATCGGCAAGTGTGATT-3'; BmorGOBP1 5'-CCCATATGGATGTCTACGTCATGAAAGATG-3' and 5'-GGAATTCTCATTTGTCCGCTTCCGATTCCA-3'; BmorGOBP2 5'-ATCATATGACCGCCGAGGTGATGAGCCACG-3'and 5'-GGAATTCTCAGTATTTTTCGATAACTGCTT-3'; BmorPBP1 5'-CAGTGGATGCGTCTCAAGAA-3' and 5'-GTCTCATCGGCTCCATGTTT-3'; BmorPBP2

15

5'-CCCATATGTCTTCAGAAGCAATGAGACACA-3'   and   5'-
GGAATTCTTATATTTCCGTCATAACTTCTC-3';   BmorPBP3   5'-
CCCATATGTCCCGAGATGTGATGACTAATC-3'   and   5'-
GGAATTCTTAGGACTTCCAAGACACCTCAT-3';   BmorABPx   5'-
CCCATATGGCACACGGTCAACTCCACGACG-3'   and   5'-
GGAATTCCTAAATGAGGAAGTAGTCCGCCT-3'.

The qRT-PCR reactions (20 ul) for each tissue were performed on an ABI 7500 (Applied Biosystems, Foster City, CA, USA) using 200 ng cDNA from each tissue and 10 uM gene specific primers. The reactions were hot-started for 2 min at 95°C, followed by 40 cycles of 95°C for 15 sec, 60°C for 30 sec and 72°C for 15 sec. Two *B. mori* reference genes, actin A4 (Genbank accession no. U49644) and elongation factor 1g (Genbank accession no. NM_001043387) were used in each qRT-PCR experiment to check loading, reverse transcriptase efficiency and the integrity of the transcripts. For each tissue qRT-PCRs were run in 6 replicates for the actin gene and 5 replicates for the elongation factor gene with two biological samples.

Quantification of relative tissue expression.

It was found that the expression levels of the reference genes varied between tissues making it impossible to have a common calibrator for comparison of the expression levels across different tissues. Therefore the 'cycle threshold' scores (Cts) of the reference genes were determined in each tissue and the relative expression levels of each gene were calculated against the expression levels of the reference gene in the same tissue. Raw Cts were converted to quantities representing relative expression levels using a modified comparative Ct method [67] with correction for different amplification efficiencies. [68] Briefly, after qRT-PCR Ct values were exported into the LinRegPCR program to correct the amplification efficiencies for each reaction. The relative expression levels (Pfaffl ratio) of each OBP gene to the reference gene were then calculated in each tissue from $[(E,obp^{\Delta Ct,obp}]/[(E,ref^{\Delta Ct,ref}]$, where E,obp and E,ref

are the corrected amplification efficiencies for the reference and OBP gene, respectively, and $\Delta Ct,obp$ is calculated from [Ct,obp of antennae-Ct,obp of body] and $\Delta Ct,ref$ is calculated [Ct,ref of antennae-Ct,ref of body]. These ratios were used to compare the relative expression levels between genes in a specific tissue. When comparing the expression levels of an OBP gene between tissues the expression levels were normalised against those of the same gene in the body.

Protein expression and purification of recombinant OBPs.

Full-length cDNAs encoding mature BmorPBP1, BmorPBP2, BmorGOBP1, BmorGOBP2 and BmorABPx were cloned into the bacterial expression vector pET17b (Novagen, Darmstadt, Germany) between the *Nde*I and *Eco*RI restriction sites. All cloned sequences were verified by sequencing and plasmids with the correct inserts were transformed into BL21(DE3)pLysS *E. coli* cells and protein synthesis induced at OD_{600} of 0.5-0.8 with IPTG (4 mM) for 3 hours. All OBPs were found to be expressed as inclusion bodies and solubilisation was performed by denaturation in urea/DTT, renaturation and extensive dialysis, using a protocol applied successfully to other OBPs [58.] The recombinant proteins were purified by two rounds of anion-exchange chromatography using a HiPrep 16/40 column (GE Healthcare) filled with DE-52 resin (Whatman), followed by gel filtration on a Suphacryl S-200 HiPrep 26/60 column (GE Healthcare). A MonoQ column was also used at the final stage of purification. The purified proteins were stored at -20°C in 20mM Tris-HCl pH 7.4 buffer.

Chemical synthesis.

The four analogues of bombykol, including bombykal were synthesized in house and the synthesis schemes are detailed in Supplementary Figure 1. NMR and GC analyses were used to confirm the structure and purity of the synthesized compounds. ^{1}H and ^{13}C NMR spectroscopy were performed using a Bruker 500 Advance NMR spectrometer with ^{1}H referenced to CDCl3 (7.25 ppm), ^{13}C to CDCl3 (77.0 ppm). Purified compounds were

analyzed on a Hewlett-Packard 5880 GC, fitted with a nonpolar HP-1 capillary column (40 m, 0.32mmID, 0.52-^{l}mfilm thickness), a cool-on-column injector and a flame ionization detector (FID). The GC oven temperature was maintained at 40°C for 1 min and then raised by 10 ^{o}C /min to 200°C and the carrier gas was nitrogen.

Fluorescence competitive binding assay.

To measure the binding of the fluorescent probe NPN to OBPs, a 2 uM protein solution (1 mL) in 20 mM Tris-HCl, pH 7.4, was titrated with aliquots of 1 mM NPN dissolved in methanol to final concentrations of 0.05–22 uM. The protein/NPN complex was excited at 280 nm and emission spectra recorded between 300 and 450 nm. The competitive binding of ligands was measured by using NPN (4 uM) as the fluorescent reporter and 0.05-7 uM concentrations of each ligand dissolved in methanol, which gave molar ratios from 0.01 to 1.61 (bombykol:NPN). The total volume of methanol in the protein solution was maintained at 21 ul (2.1%) by adding methanol without ligands. Bound ligand was evaluated from the values of fluorescence intensity assuming that the protein was 100% active, with a stoichiometry of 1:1 protein:ligand at saturation.

Cold binding assay and two-phase binding assay.

The cold binding assay was developed and detailed by Leal *et al*. [40] Each experiment was performed with at least three replicates and repeated at least twice. The binding of ligands to OBPs was quantified using GC on a HP 6890 Series GC system (Hewlett Packard, USA) with a wax column (HP-5MS, 25 m x 0.25 mm; 0.25 µm; Agilent Technologies) operated under the following temperature program: 100°C for 1 min, increased to 250°C at a rate of 10°Cmin^{-1}, and held at the final temperature for 10 min. Each sample was analysed twice. The amount of each ligand in the hexane fraction was calculated from the GC traces using a single point internal standard. The first analysis contained a known amount of internal standard and the compounds of interest and the binding of the ligand was calculated from:

Equation 1**:** Internal Response Factor (IRF) = [areaIS x amountSC]/[amountIS x areaSC],

Equation 2: amount of specific compound = [amountIS x areaSC x IRF]/areaIS,

Where, IS is the internal standard and SC is the specific compound of interest.

In the two-phase binding assay 50 ul of 20 mM Tris buffer (pH 7.0 or pH 5.0) containing protein (13 uM) was added to the 100-µl V-vial and then 20 ul of hexane containing a mixture of ligands (14 uM each) including bombykol was layered on top, which gave a molar ratio of 3:1 (protein:ligand) [higher concentrations up to 10 mM of protein were used and similar results obtained (data not shown)]. The two phases were then mixed gently, centrifuged at 13,000 x g for 10 min and then incubated at room temperature for at least 2 hours. After incubation 2 ul of the top phase containing the ligands was injected into the GC and the amount of ligand which had gone into the protein phase was determined from the GC trace using Equations 1 and 2 (above) and comparison with the results obtained before incubation and without protein.

Crystallisation and 3D structure of BmorGOBP2.

BmorGOBP2 was concentrated to 10mg/ml and co-crystalised with a ten fold excess of ligand. The GOBP2/bombykol complex was found to crystallise in Hampton screen 1, condition 6, (30% Peg 4000, 200mM MgCl$_2$, 100mM Tris pH 8.5) at 16°C and other complexes crystallised in similar conditions. Diffraction experiments were performed at the Diamond Light Source, Harwell, UK. 25% glycerol in the mother liquor was used as a cryoprotectant. The best crystals diffracted to below 2Å resolution Data were integrated in MOSFLM [69] and input into the molecular replacement workflow MrBump, [70] where the space group P3$_2$21 and search model **1DQE** were found to give the best solution using Phaser.[59] The model was refined with Refmac [71] and phenix.[72] Model building was performed with the program Coot. [73] After several rounds of refinement, the ligand was fitted to the difference map density present in the molecular cavity. Subsequent ligand structures were solved using the bombykol structure with the ligand and waters removed as a starting structure using a constant set of Rfree reflections.

References

1. Steinbrecht, R.A. (1992). Experimental morphology of insect olfaction: tracer studies, X-ray microanalysis, autoradiography, and immunocytochemistry with silkmoth antennae. Microsc. Res. Tech. 22, 336-350.

2. Steinbrecht, R.A. (1998). Odorant-binding proteins: expression and function. Ann. N. Y. Acad. Sci. 30, 323-332.

3. Laue, M., Steinbrecht, R.A. & Ziegelberger, G. (1994). Immunocytochemical localization of general odourant-binding protein in olfactory sensilla of the silkmoth *Antheraea polyphemus*. Naturwissenschaften 81, 178-180.

4. Pikielny, C.W., Hasan, G., Rouyer, F. & Rosbash, M. (1994). Members of a family of Drosophila putative odourant-binding proteins are expressed in different subsets of olfactory hairs. Neuron 12, 35-49.

5. Shanbhag, S.R., Hekmat-Scafe, D., Kim, M.S., Park, S.K., Carlson, J.R., Pikielny, C., Smith, D.P. & Steinbrecht, R.A. (2001). Expression mosaic of odourant-binding proteins in Drosophila olfactory organs. Microsc. Res. Tech. 55, 297-306.

6. Ishida, Y., Chiang V. & Leal W.S. (2002). Protein that makes sense in the Argentine ant. Naturwissenschaften. 89, 505-507.

7. Leal, W.S. (2003). Proteins that make sense. In Insect Pheromone Biochemistry and Molecular Biology, the biosynthesis and detection of pheromones and plant volatiles (Blomquist, G.J. & Vogt, R.G., eds), pp 447-476, Elsevier Academic Press, London.

8. Krieger, J., Grosse-Wilde, E., Gohl, T. & Breer, H. (2005). Candidate pheromone receptors of the silkmoth *Bombyx mori*. Eur. J. Neurosci. 21, 2167-2176.

9. Breer, H., Krieger, J. & Raming, K. (1990). A novel class of binding proteins in the antennae of the silkmoth *Antheraea pernyi*. Ins. Biochem. 20, 735-740.

10. Krieger, J., Gänssle H., Raming, K. & Breer, H. (1993). Odorant binding proteins of *Heliothis virescens*. Ins. Biochem. Mol. Biol. 23, 449-456.

11. Scaloni, A., Monti, M., Angeli, S. & Pelosi, P. (1999). Structural analysis and disulfide-bridge pairing of two odorant-binding proteins from *Bombyx mori*. Biochem. Biophys. Res. Comm. 266, 386-391.

12. Leal, W.S., Nikonova, L. & Peng, G. (1999). Disulfide structure of the pheromone binding protein from the silkworm moth, *Bombyx mori*. FEBS Lett. 24, 85-90.

13. Sandler, B.H., Nikonova, L., Leal, W.S. & Clardy, J. (2000). Sexual attraction in the silkworm moth: structure of the pheromone-binding-protein-bombykol complex. Chem. Biol. 7, 143-151.

14. Zhou, J-J., Huang, W-S., Zhang, G.A., Pickett, J.A. & Field, L.M. (2004). ''Plus-C'' odourant-binding protein genes in two Drosophila species and the malaria mosquito *An. gambiae*. Gene 327, 117-129.

15. Li, Z.X., Pickett, J.A., Field, L.M., & Zhou, J-J. (2004). Identification and expression of odorant-binding proteins of the malaria-carrying mosquitoes *Anopheles gambiae* and *Anopheles arabiensis*. Arch. Ins. Biochem. Physiol. 58, 175-189.

16. Zhou J-J., Kan Y., Antoniw J., Pickett J.A., & Field, L.M. (2006). Genome and EST analyses and expression of a gene family with putative functions in insect chemoreception. Chem. Senses. 31, 453-465.

17. Zhou, J-J., He, X.L., Pickett, J.A., & Field, L.M. (2008). Identification of odorant-binding proteins of the yellow fever mosquito *Aedes aegypti*: genome annotation and comparative analyses. Ins. Mol. Biol. 17, 147-63.

18. Vogt, R. G. & Riddiford, L. M. (1981). Pheromone binding and inactivation by moth antennae. Nature 293,161–163.

19. Robertson, H.M., Martos R., Sears, C.R., Todres, E.Z., Walden, K.K., & Nardi, J.B. (1999). Diversity of odourant binding proteins revealed by an expressed sequence tag project on male *Manduca sexta* moth antennae. Ins. Mol. Biol. 8, 501-518.

20. Krieger, J., von Nickisch-Rosenegk, E., Mameli, M., Pelosi, P., & Breer, H. (1996). Binding proteins from the antennae of *Bombyx mori*. Ins. Biochem. Mol. Biol. 26, 297-307.

21. Maida, R., Mameli, M., Müller, B., Krieger, J & Steinbrecht, R.A. (2005). The expression pattern of four odorant-binding proteins in male and female silk moths, *Bombyx mori*. J. Neurocytol. 34, 149-163.

22. Pelosi, P., Zhou, J-J., Ban, L.P. & Calvello, M. (2006). Soluble proteins in insect chemical communication. Cell Mol. Life Sci. 63, 1658-1676.

23. Györgyi, T.K., Roby-Shemkovitz, A.J. & Lerner, M.R. (1988). Characterization and cDNA cloning of the pheromone-binding protein from the tobacco hornworm, *Manduca sexta*: a tissue-specific developmentally regulated protein. Proc. Natl. Acad. Sci. USA. 85, 9851-9855.

24. Callahan, F.E., Vogt, R..G, Tucker, M.L., Dickens, J.C. & Mattoo, A.K. (2000). High level expression of "male specific" pheromone binding proteins (PBPs) in the antennae of female noctuiid moths. Ins. Biochem. Mol. Biol. 30, 507-514.

25. Vogt, R.G., Rogers, M.E., Franco, M.D. & Sun, M. (2002). A comparative study of odorant binding protein genes: differential expression of the PBP1-GOBP2 gene cluster in *Manduca sexta* (Lepidoptera) and the organization of OBP genes in *Drosophila melanogaster* (Diptera). J. Exp. Biol. 205, 719-744.

26. Picimbon, J.F. & Gadenne, C. (2002). Evolution of noctuid pheromone binding proteins: identification of PBP in the black cutworm moth, *Agrotis ipsilon*. Ins. Biochem. Mol. Biol. 32, 839-846.

27. Vogt, R.G., Rybczynski, R. & Lerner M.R. (1991). Molecular cloning and sequencing of general odorant-binding proteins GOBP1 and GOBP2 from the tobacco hawk moth *Manduca sexta*: comparisons with other insect OBPs and their signal peptides. J. Neurosci. 11, 2972-2984.

28. Krieger, J., Raming, K.& Breer, H. (1991). Cloning of genomic and complementary DNA encoding insect pheromone binding proteins: evidence for microdiversity. Biochim. Biophys. Acta. 1088, 277-284.

29. Krieger, J., Mameli, M. & Breer, H. (1997). Elements of the olfactory signaling pathways in insect antennae. Invert. Neurosci. 3, 137-144.

30. Vogt, R.G., Callahan, F.E., Rogers, M.E. & Dickens, J.C. (1999). Odorant binding protein diversity and distribution among the insect orders, as indicated by LAP, an

OBP-related protein of the true bug *Lygus lineolaris* (Hemiptera, Heteroptera). Chem. Senses. 24, 481-495.

31. Pophof, B. (2004). Pheromone-binding proteins contribute to the activation of olfactory receptor neurons in the silkmoths *Antheraea polyphemus* and *Bombyx mori*. Chem. Senses. 29, 117-125.

32. Xu, P., Atkinson, R., Jones, D.N. & Smith, D.P. (2005). Drosophila OBP LUSH is required for activity of pheromone-sensitive neurons. Neuron. 45, 193-200.

33. Syed, Z., Ishida, Y., Taylor, K., Kimbrell, D.A. & Leal, W.S. (2006). Pheromone reception in fruit flies expressing a moth's odorant receptor. Proc. Natl. Acad. Sci. USA. 103, 16538-16543.

34. Grosse-Wilde, E., Svatos, A. & Krieger, J. (2006). A pheromone-binding protein mediates the bombykol-induced activation of a pheromone receptor *in vitro*. Chem. Senses. 31, 547-555.

35. Ha, T.S. & Smith, D.P. (2006). A pheromone receptor mediates 11-cis-vaccenyl acetate-induced responses in Drosophila. J. Neurosci. 26, 8727-8733.

36. Benton, R., Vannice, K.S. & Vosshall, L.B. (2007). An essential role for a CD36-related receptor in pheromone detection in Drosophila. Nature 450, 289-293.

37. Laughlin, J.D., Ha, T.S, Jones, D.N.M. and Smith, D.P. (2008). Activation of pheromone-sensitive neurons is mediated by conformational activation of pheromone-binding protein. Cell 133: 1255-1265.

38. Maida, R., Proebstl, T. & Laue, M. (1997). Heterogeneity of odorant-binding proteins in the antennae of *Bombyx mori*. Chem. Senses. 22, 503-515.

39. Maida, R., Steinbrecht A., Ziegelberger, G. & Pelosi, P. (1993). The pheromone binding protein of *Bombyx mori*: Purification, characterization and immunochemical localization. Ins. Biochem. Mol. Biol. 23, 243-253.

40. Leal, W.S, Chen, A.M., Ishida, Y., Chiang, V.P., Erickson, M.L., Morgan, T.I. & Tsuruda, J.M. (2005). Kinetics and molecular properties of pheromone binding and release. Proc. Natl. Acad. Sci. U S A. 102, 5386-5391.

41. Leal, W.S., Chen, A.M. & Erickson, M.L. (2005). Selective and pH-dependent binding of a moth pheromone to a pheromone-binding protein. J. Chem. Ecol. 31, 2493-2499.

42. Wojtasek, H. & Leal, W.S. (1999). Conformational change in the pheromone-binding protein from *Bombyx mori* induced by pH and by interaction with membranes. J. Biol .Chem. 274, 30950-30956.

43. Lautenschlager, C., Leal, W.S., Clardy, J. (2005). Coil-to-helix transition and ligand release of *Bombyx mori* pheromone-binding protein. Biochem. Biophys. Res. Comm. 335, 1044-1050.

44. Horst, R., Damberger, F., Luginbühl, P., Güntert, P., Peng, G., Nikonova, L., Leal, W.S. & Wüthrich, K. (2001). NMR structure reveals intramolecular regulation mechanism for pheromone binding and release. Proc. Natl. Acad. Sci. USA. 98, 14374-14379.

45. Lee, D., Damberger, F.F., Peng, G., Horst, R, Güntert., P, Nikonova., L, Leal, W.S. & Wüthrich, K. (2002). NMR structure of the unliganded *Bombyx mori* pheromone-binding protein at physiological pH. FEBS Lett. 531, 314-318.

46. Damberger, F., Nikonova, L., Horst, R., Peng, G., Leal, W.S. & Wüthrich, K. (2000). NMR characterization of a pH-dependent equilibrium between two folded solution conformations of the pheromone-binding protein from *Bombyx mori*. Protein Sci. 9, 1038-1041.

47. Nakagawa, T., Sakurai, T., Nishioka, T. & Touhara, K. (2005). Insect sex-pheromone signals mediated by specific combinations of olfactory receptors. Science. 307, 1638-1642.

48. Dobritsa, A.A., van der Goes van Naters, W., Warr, C.G., Steinbrecht, R.A. & Carlson, .JR. (2003). Integrating the molecular and cellular basis of odor coding in the Drosophila antenna. Neuron. 37, 827-841.

49. Forstner, M., Gohl, T., Breer, H., Krieger, J. (2006). Candidate pheromone binding proteins of the silkmoth *Bombyx mori*. Invert. Neurosci. 6, 177-187.

50. Kaissling, K.E., Kasang, G., Bestmann, H.J., Stransky, W. and Vostrowsky, O. (1978). A new pheromone of the silkworm moth *Bombyx mori*. Naturwissenschaften 65, 382-384.

51. Butenandt, A., Beckmann, R. & Stamm, D. (1961). Über den Sexuallockstoff des Seidenspinners. II. Konstitution und Konfiguration des Bombykols. *Z. Physiol. Chem.* 324, 84–87.

52. Oldham, N.J., Krieger, J., Breer, H., Fischedick, A., Hoskovec, M. and Svatoš, A. (2000). Analysis of the silkworm moth pheromone binding protein-pheromone complex by electrospray ionization-mass spectrometry. Angew. Chem. Int. Ed. Engl., 39, 4341–4343.

53. Oldham, N.J., Krieger, J., Breer, H. & Svatos, A. (2001). Detection and removal of an artefact fatty acid from the binding site of recombinant *Bombyx mori* pheromone-binding protein. Chem. Senses 26, 529-531.

54. Zubkov, S., Gronenborn, A.M., Byeon, I.J. & Mohanty, S. (2005). Structural consequences of the pH-induced conformational switch in *A. polyphemus* pheromone-binding protein: mechanisms of ligand release. J. Mol. Biol. 354, 1081-1090.

55. Gräter, F., de Groot, B.L., Jiang, H. & Grubmüller, H. (2006). Ligand-release pathways in the pheromone-binding protein of *Bombyx mori*. Structure. 14, 1567-1576.

56. Gräter, F., Xu, W., Leal, W. & Grubmüller, H. (2006). Pheromone discrimination by the pheromone-binding protein of *Bombyx mori*. Structure. 14, 1577-1586.

57. Forêt, S. and Maleszka, R. (2006). Function and evolution of a gene family encoding odorant binding-like proteins in a social insect, the honey bee (*Apis mellifera*). Genome Res. 16(11):1404-13.

58. Zhou, J.-J., Zhang, G.A., Huang, W., Birkett, M.A., Field, L.M., Pickett, J.A., & Pelosi, P. (2004). Revisiting the odorant-binding protein LUSH of *Drosophila melanogaster*: evidence for odour recognition and discrimination. FEBS Lett. 558,23-26.

59. McCoy, A. J., Grosse-Kunstleve, R.W., Adams, P.D., Winn, M.D., Storoni, L.C. and Read, R.J. (2007). *Phaser* crystallographic software. *J*. Appl. Cryst. 40, 658-674.

60. Malnic, B., Hirono, J., Sato, T. & Buck, LB. (1999). Combinatorial receptor codes for odors. Cell. 96, 713-23.

61. Kajiya, K., Inaki, K., Tanaka, M., Haga, T., Kataoka, H. & Touhara, K. (2001). Molecular bases of odor discrimination: Reconstitution of olfactory receptors that recognize overlapping sets of odorants. J. Neurosci. 21, 6018-6025.

62. Lautenschlager, C., Leal, W.S., Clardy, J. (2007). *Bombyx mori* pheromone-binding protein binding nonpheromone ligands: implications for pheromone recognition. Structure. 15,1148-54.

63. Pesenti, M.E., Spinelli, S., Bezirard, V., Briand, L., Pernollet, J.C., Tegoni, M. & Cambillau, C. (2008). Structural basis of the honey bee PBP pheromone and pH-induced conformational change. J Mol Biol. 380, 158-169.

64. Thompson, J.D., Gibson, T.J., Plewniak, F., Jeanmougin F. & Higgins, D.G. (1997). The CLUSTAL_X windows interface: flexible strategies for multiple sequence alignment aided by quality analysis tools. Nucleic Acids Res. 25, 4876-4882.

65. Tamura, K., Dudley, J., Nei, M. & Kumar, S. (2007). MEGA4: Molecular Evolutionary Genetics Analysis (MEGA) software version 4.0. Mol. Biol. Evol. 24, 1596-1599.

66. Saitou, N. & Nei, M. (1987). The neighbour-joining method: a new method for reconstructing phylogenetic trees. Mol. Biol. Evol. 4, 406-425.

67. Pfaffl, M.W. (2001). A new mathematical model for relative quantification in real-time RT-PCR. Nucleic Acids Res. 29, 45.

68. Ramakers, C., Ruijter, J.M., Deprez, R.H. & Moorman, A.F. (2003). Assumption-free analysis of quantitative real-time polymerase chain reaction (PCR) data. Neurosci. Lett. 339, 62-6.

69. Leslie, A.G.W., (1992). Recent changes to the MOSFLM package for processing film and image plate data Joint CCP4 + ESF-EAMCB Newsletter on Protein Crystallography, No. 26.

70. Keegan, R.M. & Winn, M.D. (2007). Automated search-model discovery and preparation for structure solution by molecular replacement Acta Cryst. D63, 447-457.

71. Murshudov, G.N., Vagin, A.A. & Dodson, E.J. (1997). Refinement of macromolecular structures by the maximum-likelihood method. Acta Cryst. D53, 240-55.

72. Adams, P.D., Grosse-Kunstleve, R.W., Hung, L.W., Ioerger, T.R., McCoy, A.J., Moriarty, N.W., Read, R.J., Sacchettini, J.C., Sauter, N.K. & Terwilliger, T.C. (2002). PHENIX: building new software for automated crystallographic structure determination. Acta Cryst. D58, 1948-1954.

73. Emsley and Cowtan, (2004). Coot: model-building tools for molecular graphics. Acta Cryst. D60, 2126-2132.

Figure legends

Figure 1. Sequence alignment of OBPs identified in the *Bombyx mori* genome. The full-length OBP sequences were aligned using Clustal X 8.1 [64] with default gap-penalty parameters of gap opening 10 and extension 0.2. The numbers in parenthesis are the percentage identity of each sequence to BmorGOBP2. Residues in black are the highly

conserved (more than 80% identical over all sequences) and residues in grey are conserved to a secondary level (more than 60% but less than 80% identical over all sequences).

Figure 2. Phylogenetic relationship between Lepidopteran OBPs. The unrooted consensus tree was constructed from the multiple alignments using MEGA4 software [65] and generated with 1500 bootstrap trials using the neighbour-joining method [66] and presented with a cut off value of 65. The numbers are the bootstrap values calculated from 1500 replicates. Bmor, *Bombyx mori*; Lma, *Leucophea madderae*; Mbra, *Mamestra brassicae*; Aper, *Antheraea pernyi*; Apol, *Antheraea polyphemus*; Msex, *Manduca sexta*; Hvir, *Heliothis virescens*; Avel, *Argyrotaenia velutinana*; Cros, *Ceratitis rosa*; Cpar, *Choristoneura parallela*; Cpin, *Choristoneura pinus*; Cmur, *Choristoneura murinana*; Epos, *Epiphyas postvittana*; Pgos, *Pectinophora gossypiella*; Ofur, *Ostrinia furnacalis*; Onub, *Ostrinia nubilalis*; Aips, *Agrotis ipsilon*; Aseg, *Agrotis segetum*; Hass, *Helicoverpa assulta*; Harm, *Helicoverpa armigera*; Hzea, *Heliothis zea***;** Ldis, *Lymantria dispar*; Sexi, *Synanthedon exitiosa*; Ycag, *Yponomeuta cagnagellus*; Sfru, *Spodoptera frugiperda*; Pxyl, *Plutella xylostella*.

Figure 3. OBP transcript levels (relative to the elongation factor) in different parts of adult *Bombyx mori*, measured by quantitive real time RT-PCR (see Materials and Methods).

Figure 4. Fluorescence emission spectra of BmorGOBP2. The protein (2 uM) was excited at 280 nm and fluorescence emission spectra recorded between 310 and 455 nm. A. the emission spectra with different concentrations from 0 uM (light blue line) up to 16 uM (dark blue line) of NPN. B. The plot of peak emission at 330 nm and 395 nm against NPN concentrations.

Figure 5. Fluorescence displacement of NPN from *Bombyx. mori* OBPs by bombykol (♦)and its analogues bombykal (■), (10*E*,12*Z*)-tetradecadien-1-ol (**X**), (10*E*)-hexadecen-12-yn-1-ol

(✱), (8*E*,10*Z*)-hexadecadien-1-ol (▲) and hexandecanol (●). A. BmorGOBP2, B. BmorGOBP1, C. BmorPBP2, D. BmorPBP1, E. BmorABPx. The protein and NPN were both at 2 uM. The protein/NPN complexes were excited at 280 nm and the fluorescence emission at 395 nm was measured before and upon titration with methanol solutions of the competitors to final concentrations of 0.5-7 uM. The reductions in NPN fluorescence emission at 395 were normalised to the NPN fluorescence before titration. The decrease in NPN fluorescence intensity at the emission maximum (395-400 nm) at increasing concentrations of competitors is presented as (Fligand/Fnpn) with Fligand=the peak fluorescence intensity at a distinct competitor concentration. Fnpn=the peak fluorescence intensity of the OBP/NPN complex.

Figure 6. Displacement of the fluorescent probe NPN by bombykol and bombykal. The protein and NPN were both incubated at a concentration of 2 uM. The OBP/NPN complexes were excited at 280 nm and the fluorescence emission at 395 nm was measured before and upon titration with bombykol (white bar) or bombykal (black bar) at a final concentration of 7 uM. The reductions in NPN fluorescence emission at 395 nm were normalised to the NPN fluorescence before titration. Each column is the average of three replicates and the bar denotes the standard error.

Figure 7. Binding of bombykol and its analogues to *Bombyx. mori* OBPs as measured by A. the cold binding assay and B. the two-phase binding assay (see Materials and Methods). Each column is the average of three replicates and the bar denotes the standard error.

Figure 8. 3D structures of BmorGOBPs with ligands. **A**. Stereo view of the BmorGOBP2 liganded and apo structures. Bombykol (blue), bombykal (coral), (10*E*,12*Z*)-tetradecadien-1-ol (yellow), (10*E*)-hexadecen-12-yn-1-ol (cyan), (8*E*,10*Z*)-hexadecadien-1-ol (megenta), apo (black). The bombykol ligand is shown in sphere representation. N and C termini and periodic residues are as indicated in the right hand image. **B**. Stereo view of bombykol plus

water structure of BmorGOPB2 with the final 2Fobs-Fcal map in pink contoured at 1.0σ clipped to the ligand and water and the Fobs-Fcal map before modelling the ligand contoured at 2.3σ unclipped in green. Side chains of GOBP2 are shown in green. Ser56 and the bombykol of the SSM superposed structure of BmorPBP1 (1dqe) are shown in blue. **C**. Fobs-Fcal electron density maps (represented as blue chickenwire) for the BmorGOBP2 ligands before the ligands were added to the structure contoured at 2.3σ. i) bombykol coordinated directly to Arg110 and to the main chain carbonyl of Val66. ii) bombykol coordinated via a water. iii) bombykal, coordinated to a water which is also coordinated to Glu98. iv) (8*E*,10*Z*)-hexadecadien-1-ol, coordinated both to Glu98 and water. v) (10*E*)-hexadecen-12-yn-1-ol, coordinated to water and Glu98. vi) (10*E*,12*Z)*-tetradecadien-1-ol, coordinated to Glu98 and water. Hydrogen bonds are indicated by dashed black lines as predicted by the algorithm of the CCP4MG molecular graphics program.

Figure 9. Superposition of BmorPBP1 (pdb code:1DQE) and BmorGOBP2 to show structural differences. **A**. Stereo pair of BmorPBP1 (red), BmorGOBP2 (blue with regions of greatest difference in light blue). The disulfide bonds are yellow. The bombykol ligand is represented as cylinders and coloured light blue for the BmorGOBP2 bound conformation and pink for the BmorPBP1 bound conformation. The ligand hydrogen bonding residues Ser56 for BmorPBP1 and Arg110 for BmorGOBP2 are shown as green cylinders. **B**. i) Enlarged and simplified view of the major structural difference in the rear entry region (C-termini from residue 126 and residues 25-49). Features are coloured as described above. A potentially important stabilising hydrogen bonding network has been included for BmorPBP1 (Tyr41 and Glu32, shown as pink cylinders). The equivalent Phe41 in BmorGOBP2 (shown as blue cylinders) is more deeply buried and occupies the space of the helix in BmorPBP1. The equivalent region of BmorGOBP2 bulges out to occupy the space filled by the C-terminus of BmorPBP1. ii) Cut away view of the ligand binding pocket showing the key hydrogen bonds formed with the bombykol hydroxyl. PBP1 in red/pink and GOBP2 in blue. Hydrogen

bonding side chains in green. **C**. Schematic representation of the possible hydrogen bonding modes of bombykol and bombykal, hydrogen bonds shown as dotted lines. i) The hydroxyl of bombykol able to form two hydrogen bonds to water and Glu98 and ii) the aldehyde of bombykal only able to form a single hydrogen bond to water.

Supplementary Figure 1. Synthesis of bombykol and its analogues. The name of each analogues is given under its structure. The roman numbers in parenthesis and bold indicate steps for **(I)** Synthesis of (10E)-hexadecen-12-yn-1-ol and (10E,12Z)-hexadecadien-1-ol (bombykol) (Miyaura et al., 1983): Sonogashira coupling between 1-pentyne and (E)-11-iodoundec-10-en-1-ol, using PdCl$_2$(PhCN)$_2$ gave which was subsequently reduced to (10E,12Z)-hexadecadien-1-ol in the presence of a Zn/Cu/Ag reagent (Mcelfresh et $al.$, 1999). **(II)** Synthesis of (10E,12Z)-hexadecadienal (bombykal): Oxidation of bombykol using TPAP and NMO gave bombykal. **(III)** Synthesis of (10E,12Z)-tetradecadien-1-ol: Sonogashira coupling between 1-propyne and (E)-11-iodoundec-10-en-1-ol using PdCl$_2$(PhCN)$_2$ gave an enyne which was subsequently reduced to (10E,12Z)-tetradecadien-1-ol in the presence of a Zn/Cu/Ag reagent to give (10E,12Z)-tetradecadien-1-ol. **(IV)** Synthesis of (10E)-hexadecen-12-yn-1-ol and (8E,10Z)-hexadecadien-1-ol: (E)-9-iodonon-8-en-1-ol was obtained by the successive treatment of 8-nonyn-1-ol with Schwartz's reagent (Cp$_2$Zr(H)Cl) and iodine (Ando et al., 1982). Sonogashira coupling between 1-heptyne and (E)-9-iodonon-8-en-1-ol using PdCl$_2$(PhCN)$_2$ gave (10E)-hexadecen-12-yn-1-ol which was subsequently reduced to (8E,10Z)-hexadecadien-1-ol in the presence of a Zn/Cu/Ag reagent.

Table 1. (continue) Data Collection and Refinement Parameters for BmorGOBP2/ligand and apo-BmorGOBP2 structures.
* First two columns refer to different models of the same data set.

Parameter	Bombykol direct to Arg110 *	Bombykol via water *	Bombykal	(10*E*,12*Z*)-tetradecadien-1-ol	No ligand	(8*E*,10*Z*)-hexadecadien-1-ol	(10*E*)-hexadecen-12-yn-1-ol
Resolution (Å)	31.6-1.9 (2.0-1.9)	31.6-1.9 (2.0-1.9)	43.1-1.7(1.79-1.7)	57.5-1.4(1.48-1.4)	42.9-1.6 (1.69-1.60)	43.0-1.6 (1.69-1.6)	63.2-1.5 (1.54-1.5)
Completeness (%)	99.2(100)	99.2(100)	98.1(94.7)	94.7(89.6)	84.7(78.6)	85.1(85.5)	92.9(95.4)
Rmerge (%)	0.097(0.23)	0.097(0.23)	0.098(0.22)	0.07(0.25)	0.11(0.30)	0.07(0.32)	0.11(0.38)
I/ō	11.1(6.5)	11.1(6.5)	10.3(4.9)	13.3 (4.8)	12.5(5.9)	12.0(4.5)	14.8(3.8)
Total reflections	47846(7416)	47846(7416)	60818(6337)	126,061(12783)	91,561(13,436)	57,992(9,384)	121787(18940)
Unique reflections	9583(1903)	9583(1903)	11977(1735)	19390(2591)	13,112(1,726)	13,176(1881)	17328(2487)
Space group	P3$_2$21	P3$_2$21	P3$_2$21	P3$_2$21	P3$_2$21	P3$_2$21	P3221
Multiplicity	4.7(5.1)	4.7(5.1)	4.8(3.8)	6.0(4.6)	7.0(7.8)	4.4(5.0)	6.4(6.8)
Cell dimensions							
a (α) (Å (^{0}))	33.16 (90)	33.16 (90)	33.08 (90)	33.07 (90)	33.06 (90)	33.03 (90)	33.21 (90)
b (ß) (Å (^{0}))	33.16 (90)	33.16 (90)	33.08 (90)	33.07 (90)	33.06 (90)	33.03 (90)	33.21 (90)
c (γ) (Å (^{0}))	189.67 (120)	189.67 (120)	172.38 (120)	172.29 (120)	171.63 (120)	172.10 (120)	189.38 (120)
Beam line	DLS I04	DLS I04	DLS MI03	DLS I04	DLS I03	DLS I03	DLS I03
Resolution (Å)	31.6-1.9 (1.95-1.9)	31.6-1.9 (1.95-1.9)	28.7-1.7 (1.74-1.7)	57.5-1.4 (1.44-1.4)	42.9-1.6(1.65-1.60)	43.0-1.6(1.65-1.6)	28-1.5(1.54-1.5)
R (outer shell)	16.9(19.4)	17.1 (19.5)	18.2(23.4)	17.8(22.7)	19.5(198)	17.6(20.4)	19.7(24.7)
Rfree (outer shell)	23.5 (27.0)	23.1 (27.2)	25.4(32.4)	22.8(27.2)	27.4 (26.7)	23.1(24.2)	24.0(30.7)
Number of atoms							
Protein	1141	1141	1186	1209	1161	1189	1154
Ligand	17	17	17	15		17	17
Water	120	121	121	135	80	65	115
Magnesium	1	1	4	6	3	3	2
Wilson B Factor	14.1	14.1	16.7	12.0	16.2	17.4	14.7
Average B-factor (Å^2)							
Protein	14.7	14.7	14.8	12.8	14.5	17.1	15.4
Ligand	27.5	29.0	36.9	29.8		33.8	31.0
RMSD							
Bond angle (°)	1.8	1.8	1.9	2.0	1.9	1.8	2.0
Bond length (Å)	0.022	0.022	0.022	0.021	0.022	0.022	0.023
Ramachandran plot							
Most favoured (%)	99.3	99.3	99.2	99.2	99.2	99.2	98.5
Allowed (%)	100	100	100	100	100	100	100

Figure 1.

```
BmorGOBP1 (46%)  : -----------------------------------MWK-LVVVLTVNLLQGALTDVYVMKDVTL-----------GFG :  31
BmorGOBP2 (100%  : -----------------------------------MFSFLILVFVASVADSVIGTAEVMSHVTA-----------HFG :  32
BmorPBP1  (31%)  : ---------------------------------MSIQGQIALALMVYMAVGSVDASQEVMKNLSL-----------NFG :  35
BmorPBP2  (33%)  : -------------------------------MKLQ-----VVLVVVLTVEMVCGSRDVMTNLSI-----------QFA :  30
BmorPBP3  (33%)  : -------------------------------MARYN--IVVAVLVLGVVGARGSSEAMRHIAT-----------GFI :  33
BmorABPx  (13%)  : ----------------------------------MAVHIFLILASYMALAAHGQLDDEIAE-----------LAA :  30
BmorOBP1  (9%)   : ------------------------------------------------------MSRQQLKN-----------SGK :  11
BmorOBP2  (8%)   : ----------MKSKTKRARENRQTANMAVSEISRILTFLTIVSFIYIVYSFKPLTKDEHIERYNKMNEDIE-------PFR :  64
BmorOBP3  (15%)  : ------------------------------MFYPFRFTLLFYGLFVIYLVRAEPEKENHFTL-----------ALK :  35
BmorOBP4  (13%)  : ------------------------------------------MTSAKTDVEIKAWFLG---------------- :  16
BmorOBP5  (9%)   : ----------------------------------MYTNFILIFYFGISIYDVRASSLDDLKMVY--------------K :  31
BmorOBP6  (8%)   : MSIKWRHIERVGSFCYLGSIVDDRGGTEADIAARINKARAAFSQLRPVWSSSTLTRRTKALTEEQKAEITK-------SSL :  74
BmorOBP7  (8%)   : ------------------------------MANLVLLLTFVLMTLSMARLKSTEAPKSKTALFNDQDNMGYEELDME :  47


BmorGOBP1 (46%)  : QALEQCREESQLTEEKMEEFFHFWNDDFKFEHRELGCAIQCMSRHFNLLTDSSRMHHENTDKF-IKSFPNGEILSQKMIDM : 111
BmorGOBP2 (100%  : KTLEECREESGLSVDILDEFKHFWSDDFDVVHRELGCAILCMSNKFSLMDDDVRMHHVNMDEY-IKGFPNGQVLAEKMVKL : 112
BmorPBP1  (31%)  : KALDECKKEMTLTDAINEDFYNFWKEGYEIKNRETGCAIMCLSTKLNMLDPEGNLHHGNAMEF-AKKHGADETMAQQLIDI : 115
BmorPBP2  (33%)  : KPLEACKKEMGLTETVLKDFYNFWIEDYEFTDRNTGCAILCMSKKLELMDGDYNLHHGKAHEF-ARKHGADETMAKQLVDL : 110
BmorPBP3  (33%)  : RVLDECKQELGLTDHILTDMYHFWKLDYSMMTRETGCAIICMSKKLDLIDGDGKLHHGNAQAY-ALKHGAATEVAAKLVEV : 113
BmorABPx  (13%)  : MVRENCADESSVDLNLVEKVN-AGTDLATITDGKLKCYIKCTMETAGMMSDG----VVDVEAV-LSLLP--DSLKTKNEAS : 103
BmorOBP1  (9%)   : MLKKQCMGKNDVTEEEIGDIE----KGKFIEQKNVMCYIACTYQMTQIIKNNKISYEASIKQI-DLMYP--PELKESAKAS :  85
BmorOBP2  (8%)   : KNLTECARQVKASMADVEKFL----KRIPQSNMEGKCFVACILKRNSLIKNNKLSQENLLEVN-RAVYGDDSEVMSRLKTA : 140
BmorOBP3  (15%)  : KTLFSTARSCMSHVNANETDLEYLRKDPPFPDK-AACIIKCLLEKIGVKNNKYSKMGFLTAV-SPLVFTNKKKLDHYKSV : 114
BmorOBP4  (13%)  : -QAVECSKDHPVTTEELRMHK-----HELPDSKNAKCLMKCVFRKCNWLDSKGMYDINAAYASSTKDFSDDKTKQENANKL :  91
BmorOBP5  (9%)   : NVLKECVGDYPLTAADLKLIK-----ARQIPNDDIKCVFACAYKKTGMMTEEGMLSVEGIKDMSQKYLSDNPEQLRKSKEF : 107
BmorOBP6  (8%)   : PLLAECSKEFSVNQGDIDAAK-----KLGDPSGLNSCFVGCFMKKAGLINASGLFDVAATIEK-SKKYLTSEEDLKAFEKL : 149
BmorOBP7  (8%)   : EILVSACNESFRLEYAYLESLNDS-GSFPDETDKTPKCYIRCVLEKTELLSENGVLNPATAALVFAGERN--GKPMSDLEEM : 125


BmorGOBP1 (46%)  : IHTCEKKFDSEP----DHCWRILRVAECFKDACNKSGLAPSMELILAEFIMESEADK---------------------- : 164
BmorGOBP2 (100%  : IHNCEKQFDTET----DDCTRVVKVAACFKKDSRKEGIAP--EVAMIEAVIEKY------------------------- : 160
BmorPBP1  (31%)  : VHGCEKSTPAND----DKCIWTLGVATCFKAEIHKLNWAPSMDVAVGEILAEV----------------------- : 164
BmorPBP2  (33%)  : IHGCSQSVATMP----DECERTLKVAKCFIAEIHKLKWAPDVELLMAEVLNEVSWKS-------------------- : 163
BmorPBP3  (33%)  : IHGCEKLHESID----DQCSRVLEVAKCFRTGVHELHWAPKLDVIVGEVMTEI----------------------- : 162
BmorABPx  (13%)  : LKKCDTQKGS------DDCDTAYLTQICWQAANKADYFLI------------------------------------ : 137
BmorOBP1  (9%)   : AGRCKDVSKKYK----DICEASYWTAKCMYEDNPKDFIFA----------------------------------- : 121
BmorOBP2  (8%)   : ILECSKIVEDIF----EICEYASVFNDCMHMKMEHILDKITMERRMEALGQMSSNPDEWSEEEDEMLKLVKDEL------- : 210
BmorOBP3  (15%)  : SENCEKEINHDQT---TECELGNEVVSCIFKYAPELHFKT---------------------------------- : 151
BmorOBP4  (13%)  : FDTCKSVNEENVGDGEEGCDRSLLLAKCLTKAAPQFGFQL-------------------------------- : 131
BmorOBP5  (9%)   : AEACSSVNDQQVSDGTKGCERAALIFKCSTEKITNVMTAMRTPRRTVAADASSHPPGVGVVSTPSGRPHHREETPGFGFEL : 188
BmorOBP6  (8%)   : TETCAPENDKPVSDSDKGCERAKLLLDCFVANKGSNTRIVALSKDLDEEAEDRAQWLAIGEAYVQQ-------------- : 215
BmorOBP7  (8%)   : AVACADRHEKCK------CEKAYNFVKCLMYMEIDKYEKKN------------------------------------ : 160
```
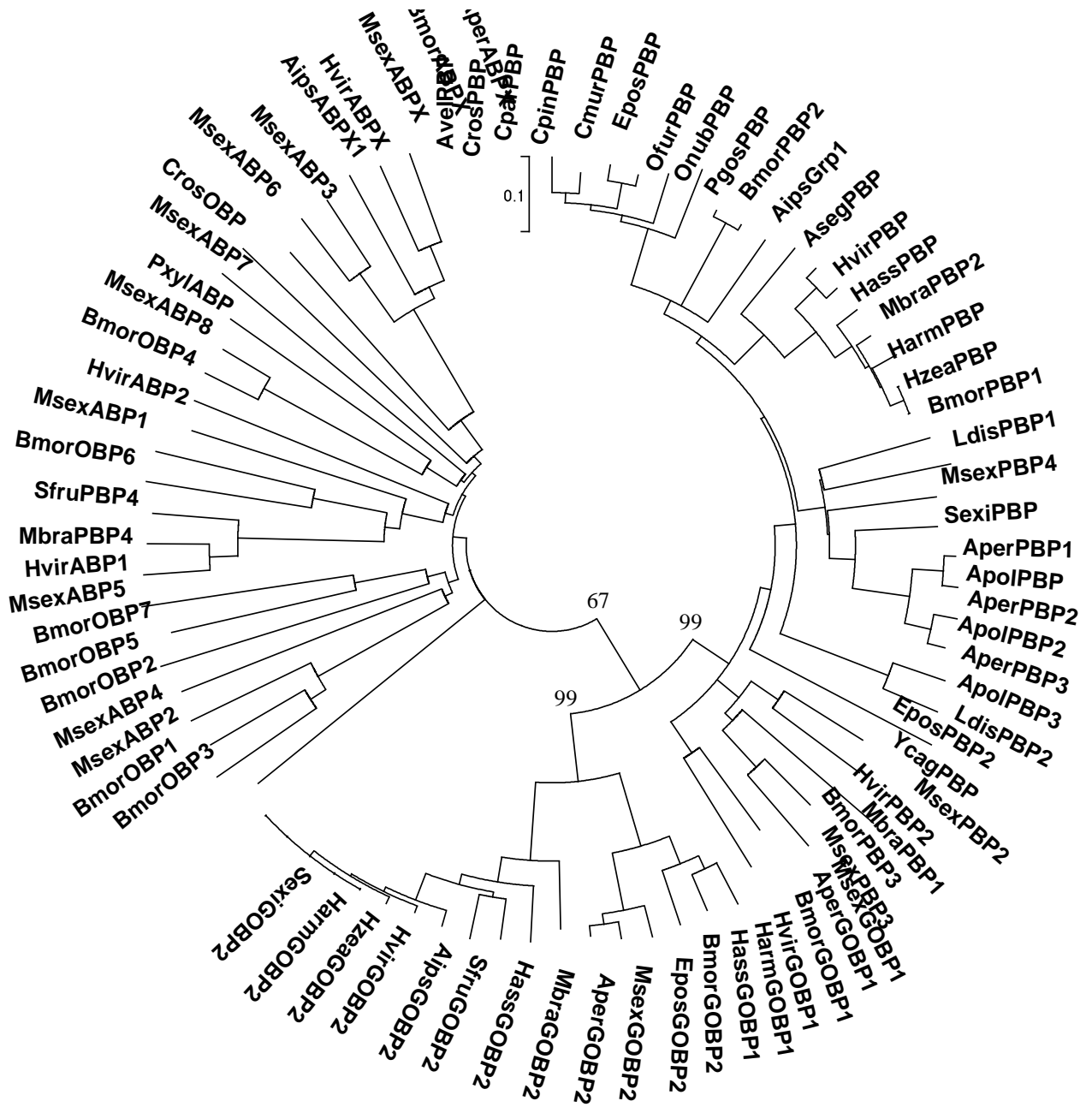
Figure 2.

Figure 3.
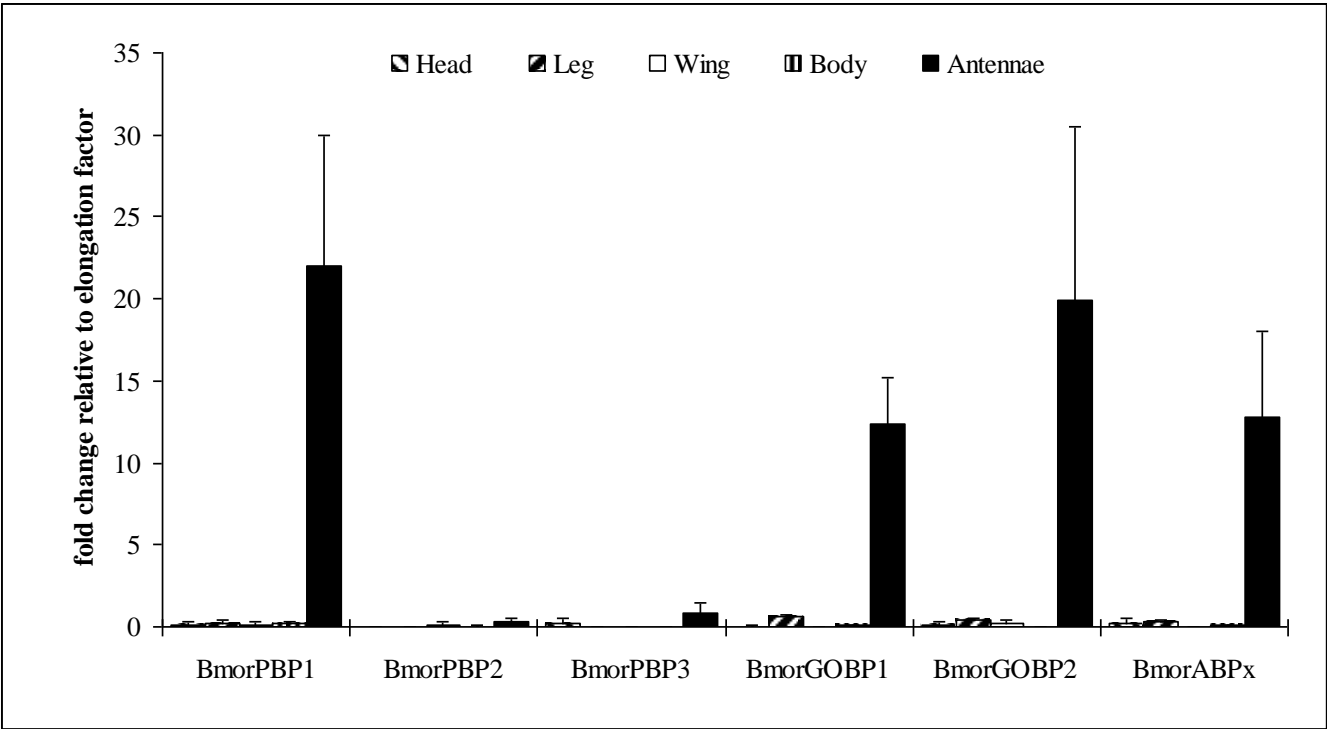
Figure 4.

A.
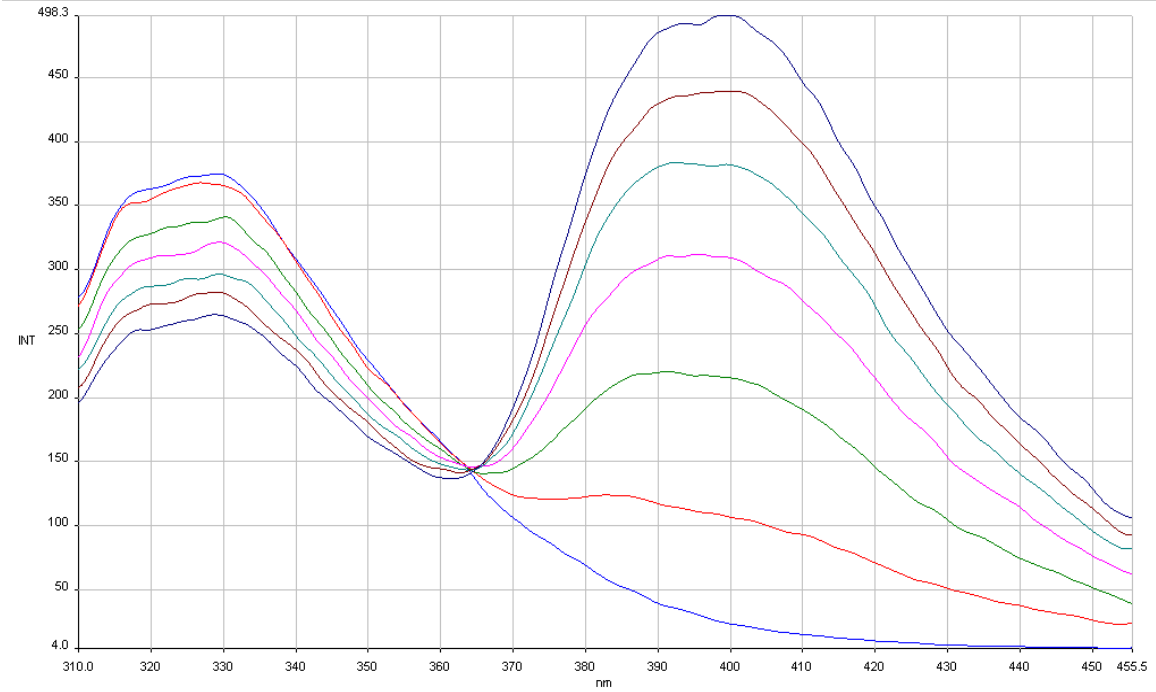
B.
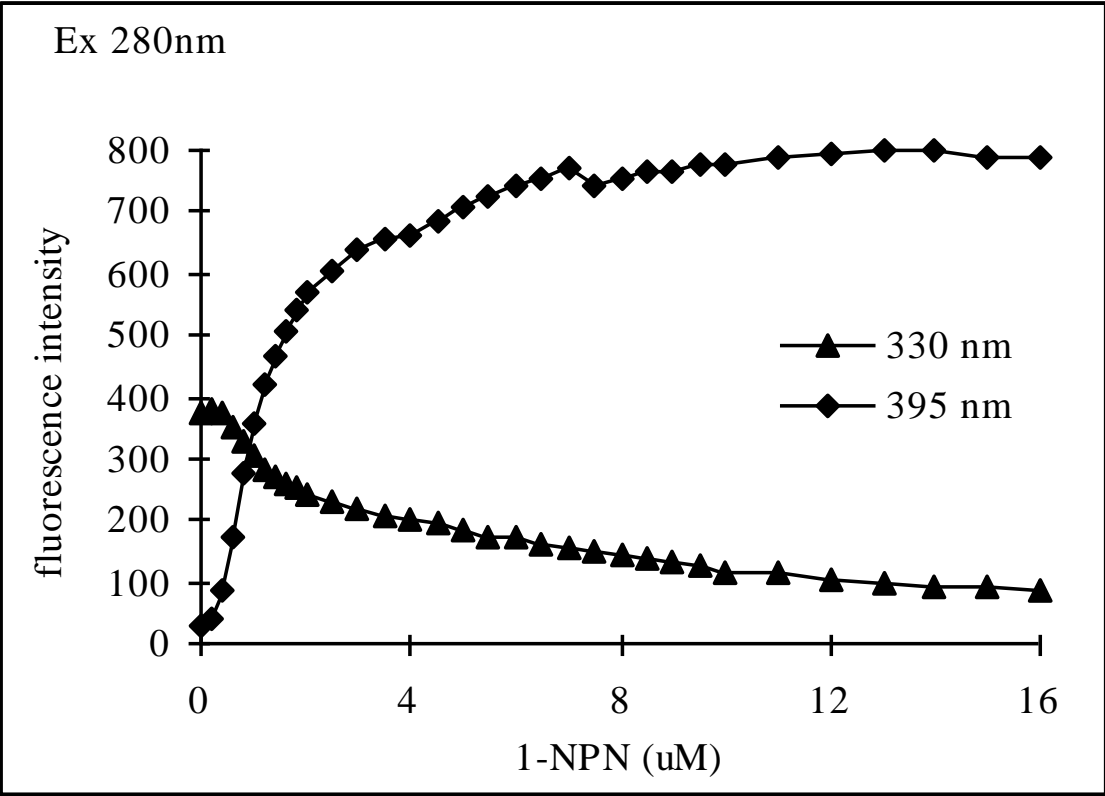
Figure 5.

A.
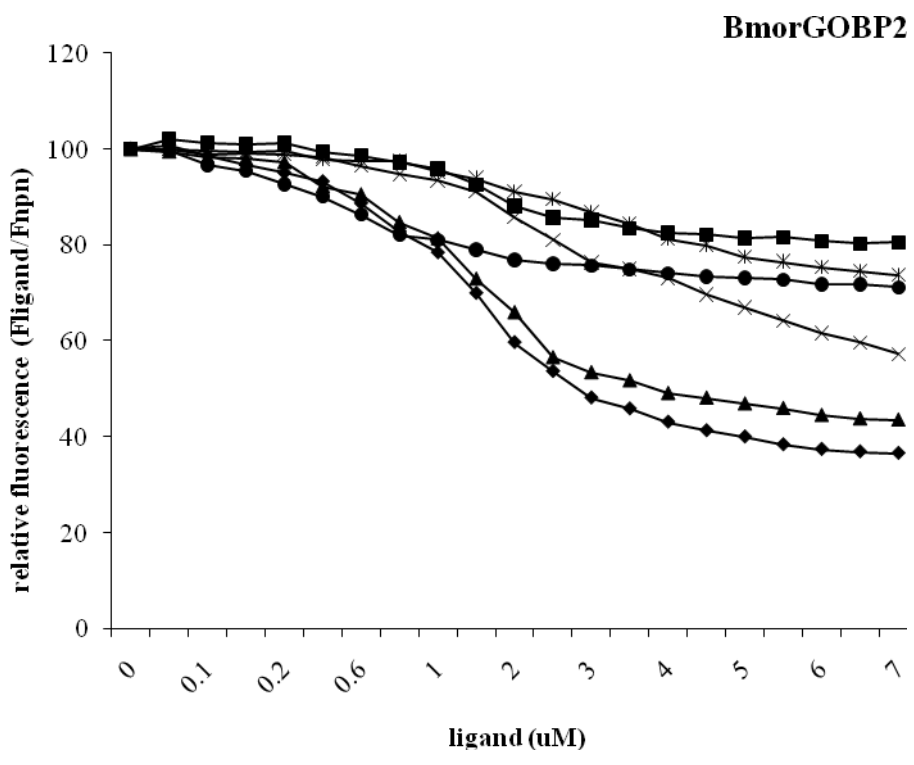
B.
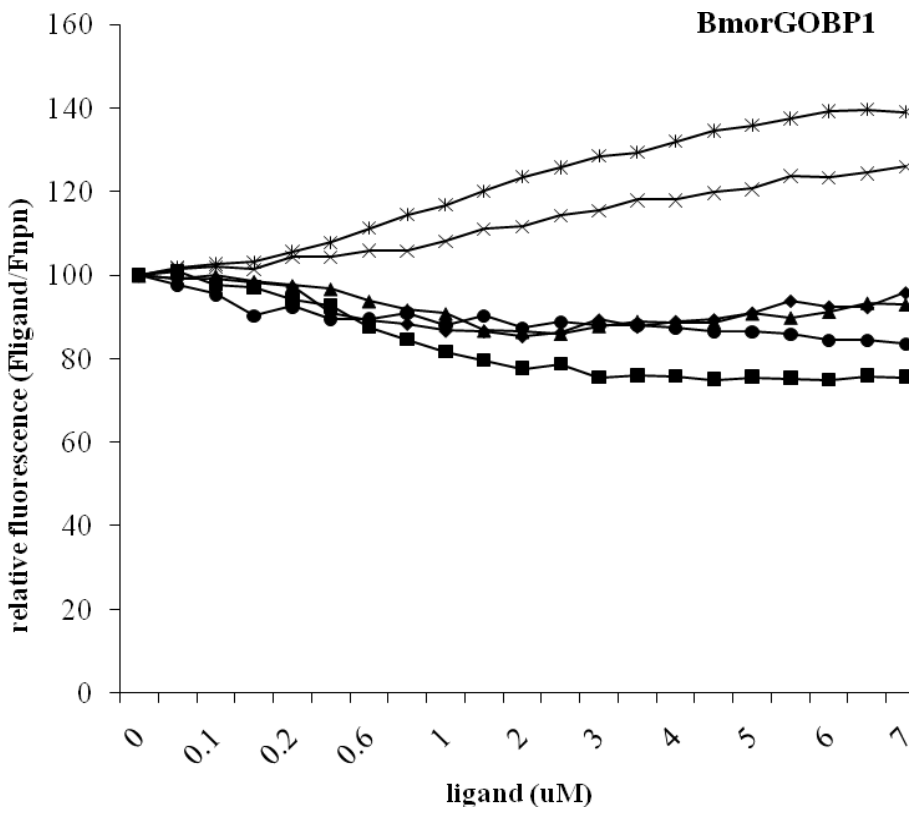
Figure 5. (cont.)

C.
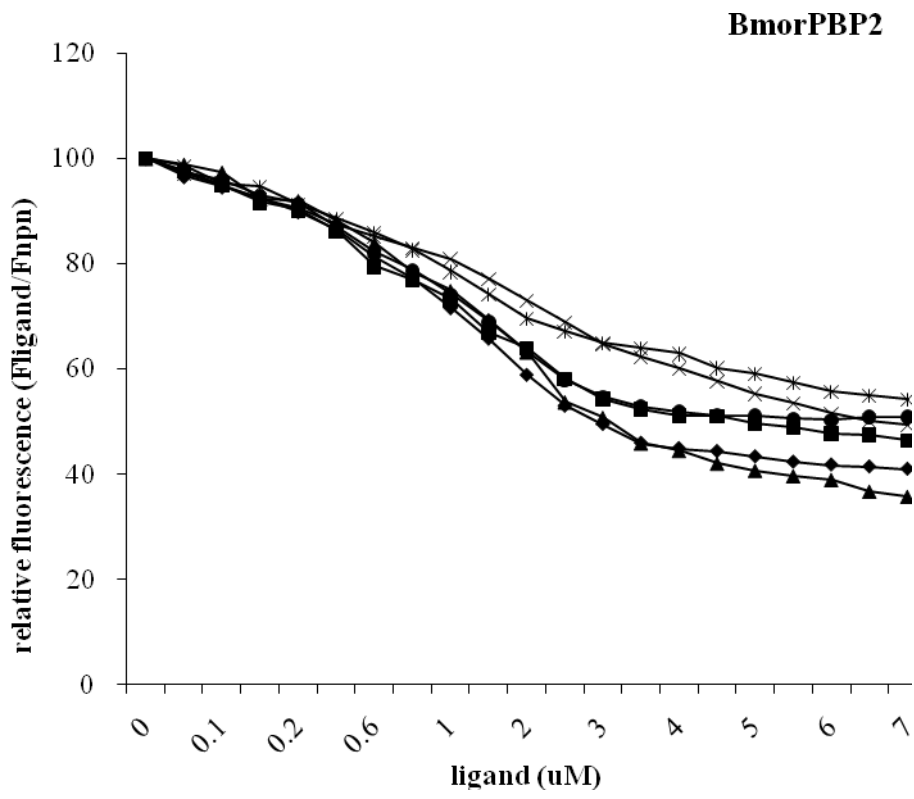
D.
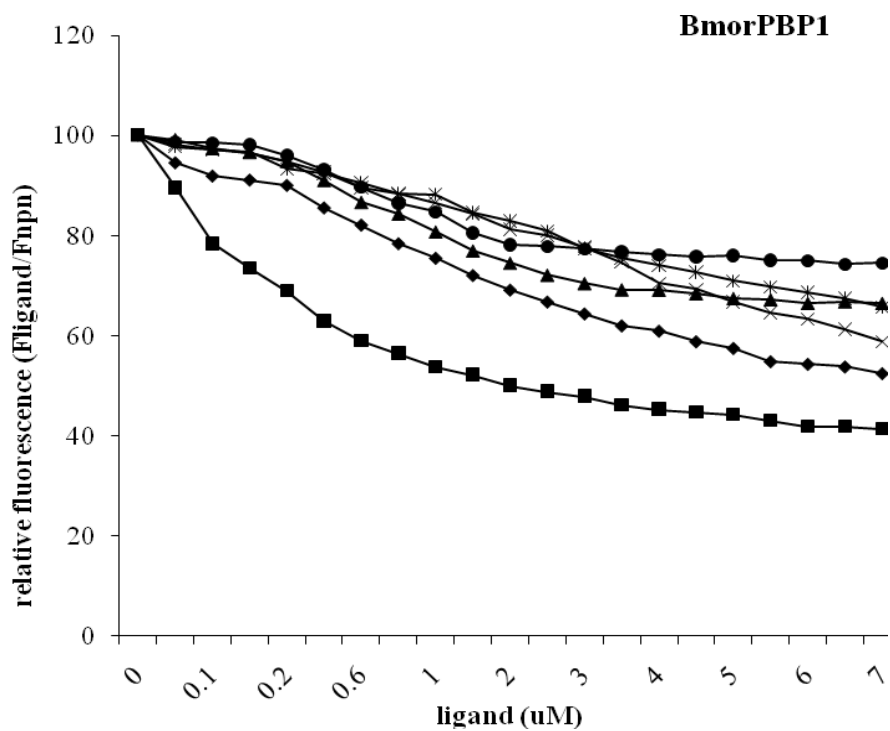
Figure 5. (cont.)

E.
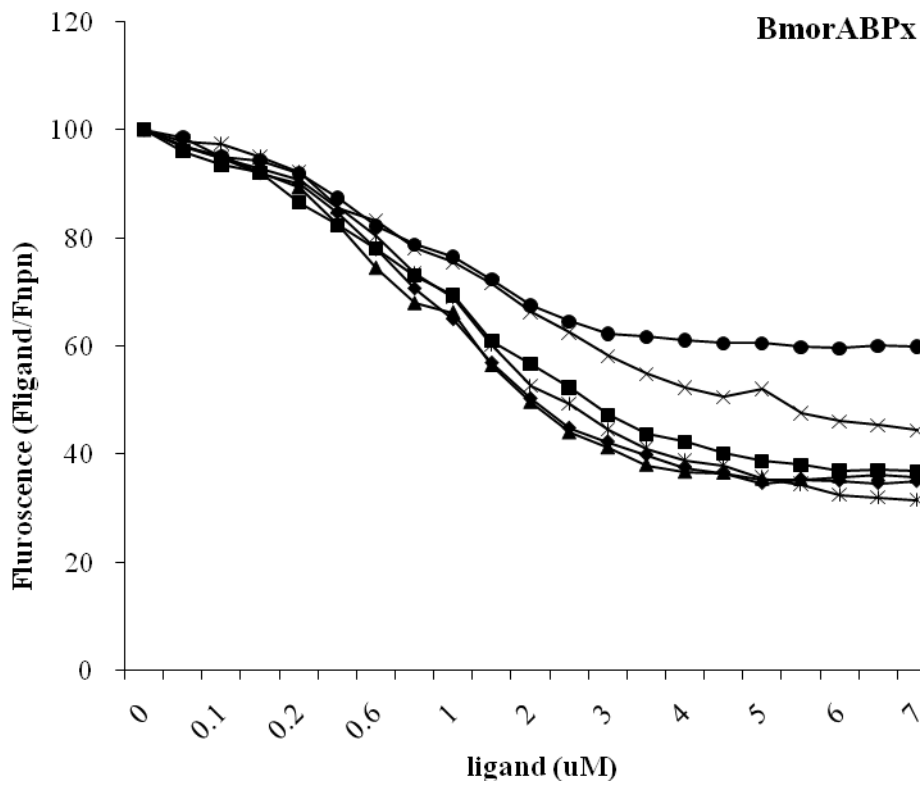
Figure 6.
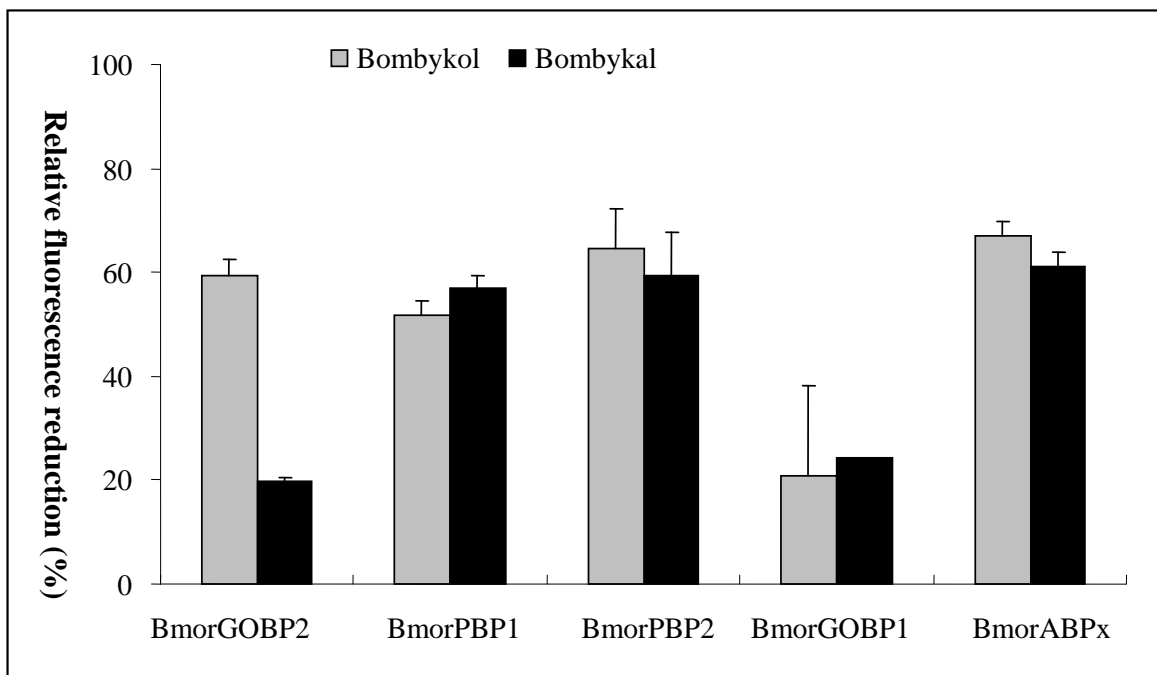
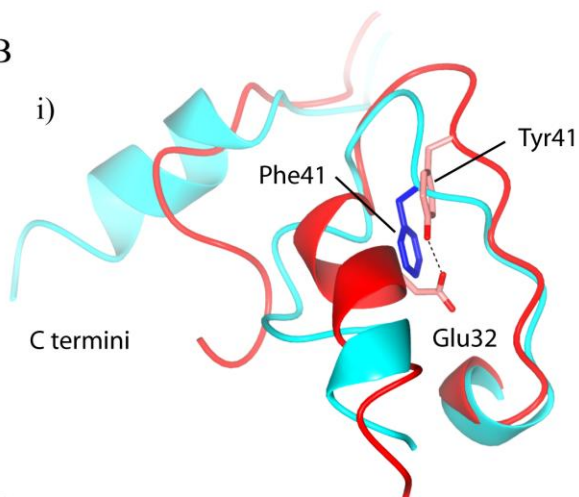**Figure 7.**

A.
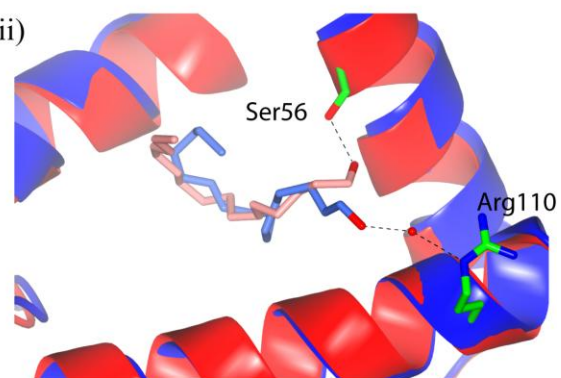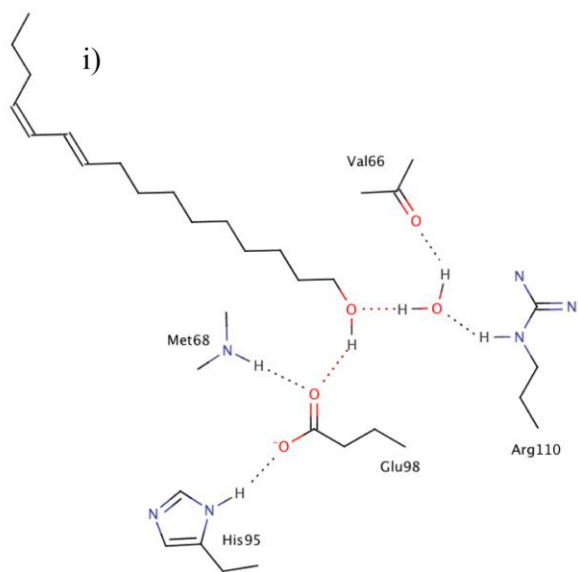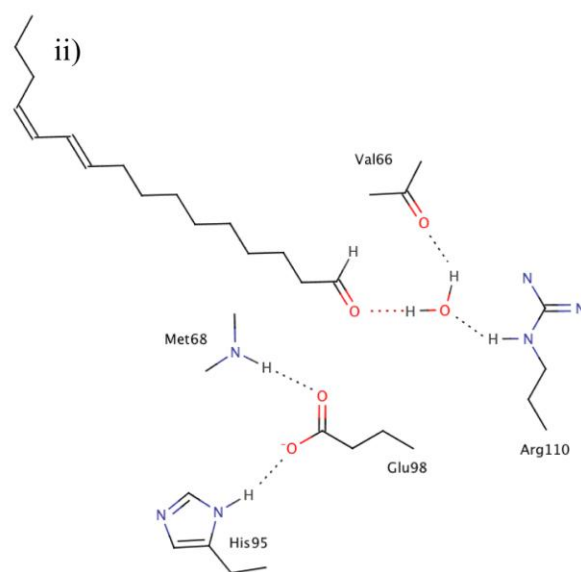

B.

Figure 8.

A

i)
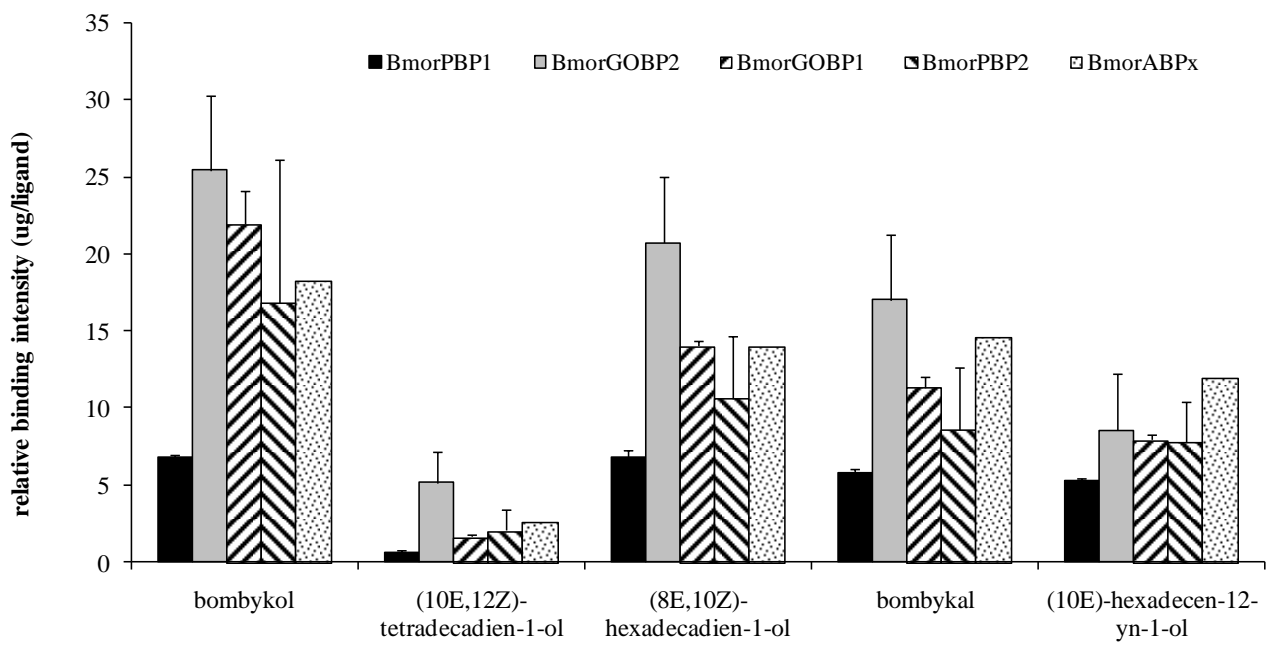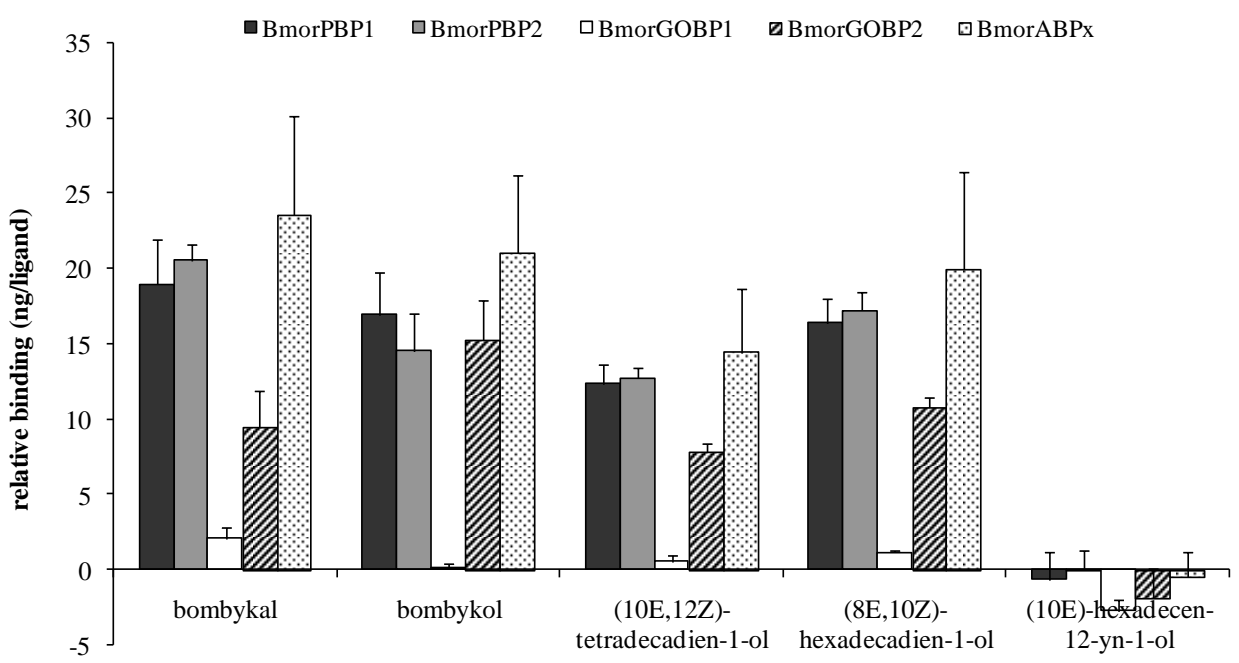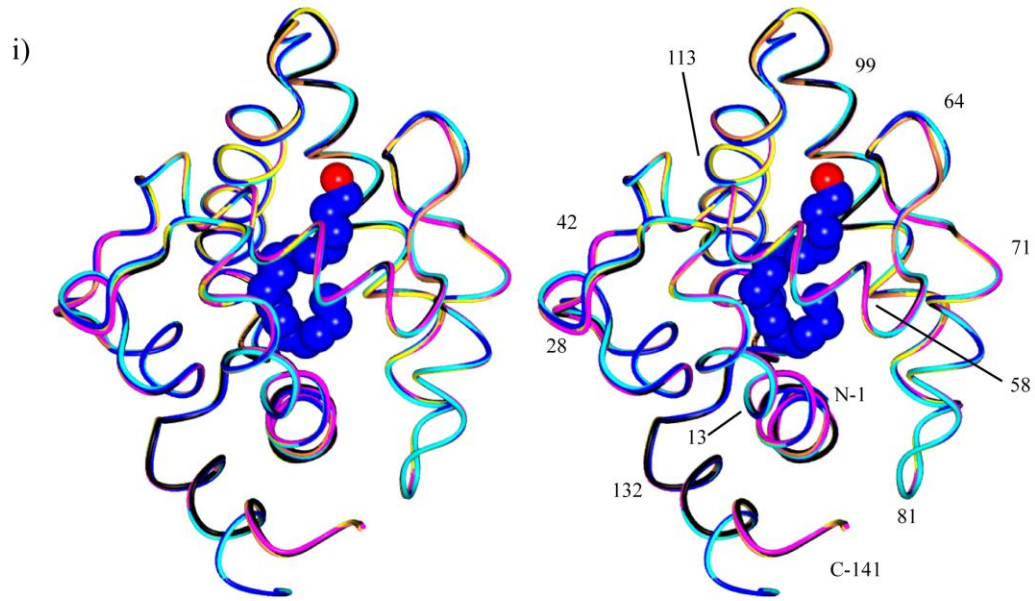
B
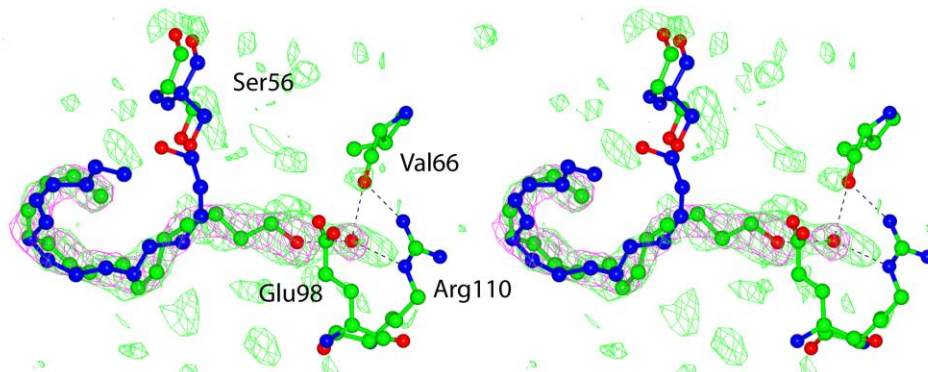
C
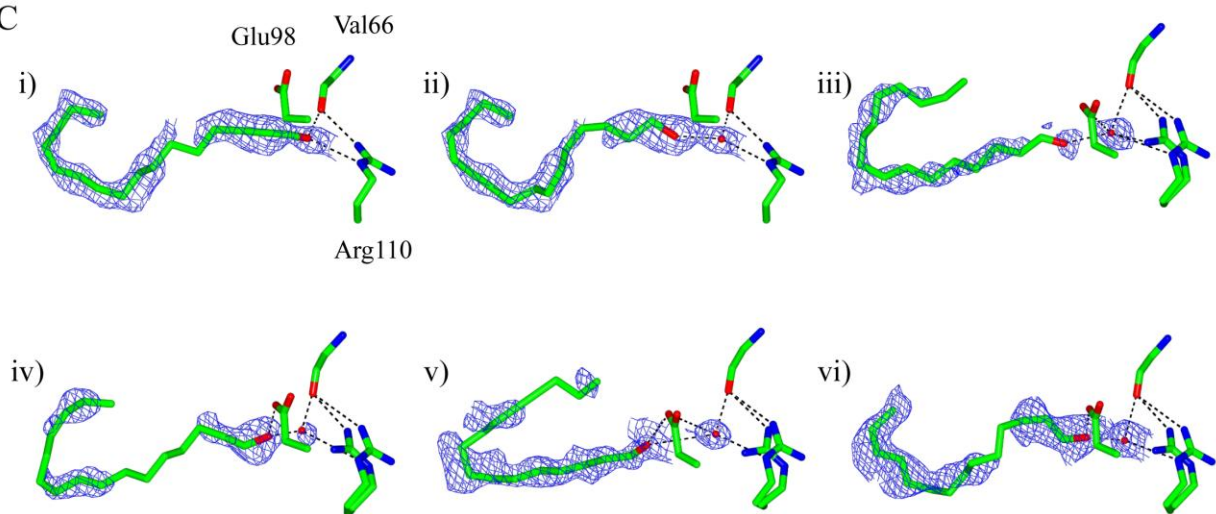
Figure 9

A

i)
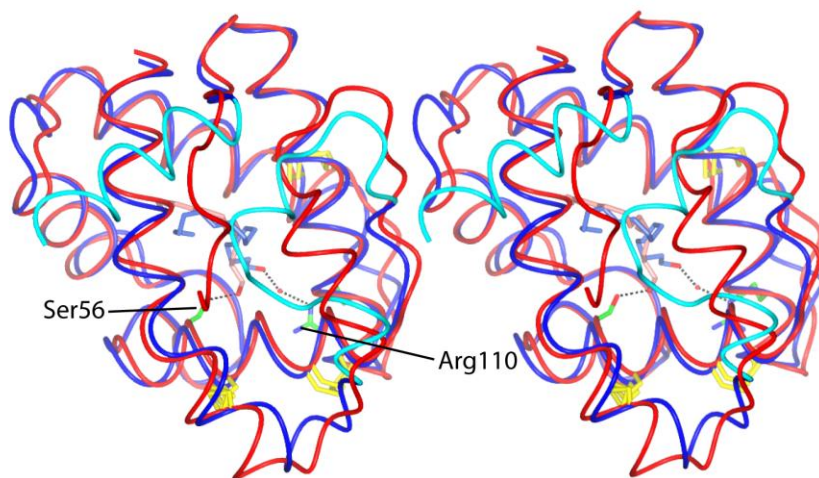
B

i)

ii)

C

i)

ii)

Supplementary Figure 1

(I) ... → **(10E)-hexadecen-12-yn-1-ol** 86% ... → **bombykol** 82%

(reagents: PdCl$_2$(PhCN)$_2$, CuI, piperidine, pentyne; then Zn/Cu(OAC)$_2$, AgNO$_3$)

(II) ... → **bombykal** (reagents: TPAP, NMO)

(III) ... → 76% ... → **(10E,12Z)-tetradecadien-1-ol** 56%

(reagents: PdCl$_2$(PhCN)$_2$, Propyne; then AgNO$_3$, Zn, Cu(OAc)$_2$)

(IV) Cp$_2$ZrCl$_2$ → (Super Hydride, THF, 1 hour) → Cp$_2$Zr(H)Cl + Et$_3$BH → (Nonynol) → ... → (I$_2$) → 81% ...

... → (PdCl$_2$(PhCN)$_2$, CuI, piperidine, heptyne) → 80% ... → (Zn, AgNO$_3$, Cu(OAc)$_2$) → **(8E,10Z)-hexadecadien-1-ol**